

Aus der Kinderklinik und Kinderpoliklinik im
Dr. von Haunersches Kinderspital
Klinik der Ludwig-Maximilians-Universität München

Direktor: Prof. Dr. med. Christoph Klein

Induction of T-cell responses against mutation-specific peptides from malignant pediatric brain tumor samples

Dissertation
zum Erwerb des Doktorgrades der Medizin
an der Medizinischen Fakultät
der Ludwig-Maximilians-Universität zu München

vorgelegt von
Milan Cedric Paul
aus Heidelberg
2020

Mit Genehmigung der Medizinischen Fakultät
der Universität München

Berichterstatter: Prof. Dr. Tobias Feuchtinger

Mitberichterstatter: PD Dr. Reinhard Obst
PD Dr. Hanna-Mari Baldauf
Prof. Dr. Peter Bartenstein

Mitbetreuung durch die
promovierte Mitarbeiterin: Dr. Franziska Blaeschke

Dekan: Prof. Dr. med. dent. Reinhard Hickel

Tag der mündlichen Prüfung: 26.05.2020

List of tables, figures and abbreviations

Tables

Table 1: Antibodies for different staining conditions in DC maturity proof.	19
Table 2: Antibodies for ICS conditions.	22
Table 3: Characteristics of two pediatric medulloblastoma patients.	24
Table 4: Detected DNA and RNA variants from NGS and deep sequencing.	26
Table 5: DNA and RNA sequencing data of both next generation and deep sequencing runs.....	27
Table 6: Characteristics of variants detected by whole exome sequencing in the two patients.....	28
Table 7: Function of mutated genes without predicted epitopes.	29
Table 8: Data of <i>in silico</i> binding-affinity prediction of all synthesized mutation-specific peptides.	31
Table 9: Overview of donor/peptide combinations tested for <i>de novo</i> T-cell responses.....	61

Figures

Fig. 1: Interaction between CD4 ⁺ helper T cells and APCs.	6
Fig. 2: Concept of adoptive T-cell transfer.	11
Fig. 3: Distribution of childhood cancer diagnoses per year.	13
Fig. 4: Experimental design: Induction of neoantigen-specific <i>de novo</i> T-cell responses.....	18
Fig. 5: Conditions of ICS panel.	21
Fig. 6: Workflow: Algorithm for identification of tumor-specific neoantigens.....	25
Fig. 7: High expression of CD80, CD83 and CD86 indicated maturity of DCs.	33
Fig. 8: Example of flow-cytometric analysis of DCs on day 11 and comparison to PBMCs. Adapted from Blaeschke, Paul <i>et al.</i> (2019)	34
Fig. 9: Example of successfully induced T-cell response (peptide 17) measured by flow cytometry.	35
Fig. 10:	36
Fig. 11: Positive T-cell responses defined by CD3 ⁺ cells only or CD4 ⁺ /CD8 ⁺ subpopulations.....	37
Fig. 12: Strong T-cell response against peptide 17 in flow-cytometric analysis.	38
Fig. 13: Proportion of IFN- γ and TNF- α release of CD4 ⁺ and/or CD8 ⁺ subpopulation in positive T-cell responses.	38
Fig. 14: Determining T-cell phenotypes.	39
Fig. 15: T-cell differentiation on final ICS.	39

Abbreviations

AF	Allele frequency
ALL	Acute lymphoblastic leukemia
APC	Antigen-presenting cell
ATT	Adoptive T-cell transfer
CAR	Chimeric antigen receptor
CD	Cluster of differentiation
CEA	Carcinoembryonic antigen
CGAs	Cancer-germline antigen
CLL	Chronic lymphocytic leukemia
CM	Central memory
CNS	Central nervous system
CTL	Cytotoxic T cell
CTLA-4	Cytotoxic T lymphocyte-associated antigen 4
DC	Dendritic cell
DMSO	Dimethyl sulfoxide
EDTA	Ethylenediaminetetraacetic acid
EM	Effector memory
FACS	Fluorescence-activated cell sorting
FC	Fold change
FMO	Fluorescence minus one
FSC	Forward scatter
GM-CSF	Granulocyte-macrophage colony-stimulating factor
HAL	Histidine ammonia-lyase
HER2	Human epidermal growth factor receptor 2
HLA	Human leukocyte antigen
HSA	Human serum albumin
ICS	Intracellular cytokine staining
IFN- γ	Interferon gamma
IL	Interleukin
MAX	MYC associated factor X
MB	Medulloblastoma
MHC	Major histocompatibility complex
mo-DC	Monocyte-derived DC
MUC4	Mucin 4
NEU2	Neuraminidase 2
NGS	Next generation sequencing
NK	Natural killer
PAPD5	PAP associated domain containing 5
PBL	Peripheral blood lymphocyte
PBMC	Peripheral blood mononuclear cell
PBS	Phosphate buffer saline
PCSK9	Proprotein convertase subtilisin
PD-1	Programmed cell death protein 1
PDCD10	Programmed cell death 10

PD-L1	Programmed cell death 1 ligand 1
PGE2	Prostaglandin E2
PI3K	PIK3CA-derived protein phosphoinositide 3-kinase
PIK3CA	Phosphatidylinositol-4,5-bisphosphate-3-kinase catalytic subunit alpha
PMA	Phorbol-12-myristate-13-acetate
PTEN	Phosphatase and tensin homolog
RCF	Relative centrifugal force
RT	Room temperature
SCM	Stem cell memory
SSC	Side scatter
SHH	Sonic hedgehog
SNV	Single nucleotide variant
TAA	Tumor-associated antigen
TCR	T-cell receptor
Th1	Type 1 helper T cell
TIL	Tumor-infiltrating lymphocyte
TNF- α	Tumor necrosis factor alpha
Treg	Regulatory T cell
TSA	Tumor-specific antigen
TSEN54	tRNA splicing endonuclease subunit 54
VEGF	Vascular endothelial growth factor
WES	Whole exome sequencing
WTS	Whole transcriptome sequencing

Content

A	Introduction	6
1	Role of the immune system in tumorigenesis.....	6
1.1	Antigens with low tumor specificity	7
1.2	Antigens with high tumor specificity	7
1.3	The concept of immunoediting.....	8
1.3.1	Elimination	8
1.3.2	Equilibrium and escape	9
2	Immunotherapy as a fourth pillar of cancer treatment	10
2.1	Peptide vaccination	10
2.2	Adoptive T-cell transfer	11
3	Medulloblastoma, the most common malignant brain tumor in childhood	12
3.1	Classification and pathogenesis	13
3.2	Therapy	14
4	Objective: Inducing a <i>de novo</i> immune response against tumor-derived peptides	14
B	Materials and Methods	15
1	Materials	15
1.1	Equipment and software	15
1.2	Solutions, media and sera for cell culture	15
1.3	Buffers and cell culture medium.....	16
1.4	Consumables.....	16
1.5	Antibodies	17
2	Methods	18
2.1	Induction of a mutation-specific <i>de novo</i> immune response.....	18
2.1.1	Generation of DCs and PBLs.....	18
2.1.2	Harvest of DCs, peptide loading and coculture of DCs and PBLs	19
2.1.3	Maturity proof of DCs.....	20
2.1.4	Weekly restimulations with autologous peptide-loaded PBMCs.....	20
2.1.5	Quantification of IFN- γ and TNF- α release <i>via</i> flow cytometry.....	21
2.2	Determination of positive T-cell responses.....	22
2.3	General cell culture	22
2.3.1	Counting cells.....	22
2.3.2	Freezing and thawing cells	22
2.4	Prediction of HLA binding affinity	23
2.5	Statistics	23
C	Results	24
1	Preliminary work: Selection and generation of tumor-specific peptides derived from medulloblastoma	24
1.1	Patients' characteristics	24
1.2	Detection of tumor-specific variants by next generation and deep sequencing	26
1.3	Identification of HLA-binding candidates <i>via</i> affinity prediction databases.....	32
2	Induction of neoantigen-specific T-cell responses <i>in vitro</i>	33
2.1	Flow-cytometric analyses of CD80, CD83 and CD86 indicate DC maturity	33
2.2	Successful induction of <i>de novo</i> T-cell responses against 9/19 medulloblastoma-derived peptides.....	33
2.3	Mutation-specific T-cell responses were mainly caused by CD8 ⁺ IFN- γ secreting cells.....	36
2.3.1	SVIL-derived peptide 17 induced strongest T-cell response	39
2.4	Impact of T-cell phenotype on induction of mutation-specific T-cell responses	39

D	Discussion	41
1	“Reverse immunology” for identification of tumor-specific neoepitopes.....	41
2	DCs are crucial for <i>de novo</i> T-cell responses and for immune regulation	43
3	CD4+ and CD8+ T cells play ambiguous roles in eliciting T-cell responses.....	43
4	Several immunogenic peptides are derived from genes with potential impact on tumorigenesis	44
5	Future therapeutic approaches include peptide vaccination and adoptive T-cell transfer	46
5.1	Impact of T-cell subsets and differentiation in ATT	48
6	Conclusion and outlook	48
E	Summary / Zusammenfassung	50
F	References	52
G	Appendix.....	61
1	Supplementary data	61
2	Acknowledgements	62
3	Eidesstattliche Versicherung.....	63

A Introduction

1 Role of the immune system in tumorigenesis

Benign as well as malignant tumors are characterized by a variety of uncontrolled features (1). The immune system plays an important role to prevent the tumorigenic process: By constantly screening the body cells and eliminating altered ones it is supposed to ensure tissue integrity which is compromised not only by infected but also by tumor cells. Immune responses of the adaptive immune system are mediated by B and T lymphocytes (2). B lymphocytes (B cells) are associated with humoral immunity: Pathogens are neutralized by molecules such as antibodies which are found in extracellular fluids. In contrast, T lymphocytes (T cells) are part of the cell-mediated immunity: T cells themselves are involved in recognizing tumor or infected cells. They are divided into helper T cells ($CD4^+$ cells) and cytotoxic T cells (CTLs; $CD8^+$ cells). $CD4^+$ cells detect foreign antigens in the extracellular compartment and help mediating immune responses by activating the innate immune system, B cells as well as CTLs (3-5). Nevertheless, they are also crucial for immunosuppressive mechanisms (6). $CD8^+$ cells can recognize altered body cells due to viral or bacterial infection or malignancy and can eliminate those cells directly. Either way, recognition arises by interaction between the T-cell receptor (TCR) on the T cells and the major histocompatibility complex (MHC) on the target cell (Fig. 1). MHC class I is found on all nucleated body cells and screened by $CD8^+$ cells whereas MHC class II is located on antigen-presenting cells (APCs) and interacts with $CD4^+$ cells (7, 8). Small peptides derived as particles of proteins either found extracellularly (MHC class II) or derived of proteins synthesized in the cytosol of body cells (MHC class I) are constantly presented on MHC molecules (9). MHC class I binds peptides of 8 – 10 amino acids (10), MHC class II of 11 – 30 amino acids (11). These MHC-peptide complexes can be recognized by TCRs in

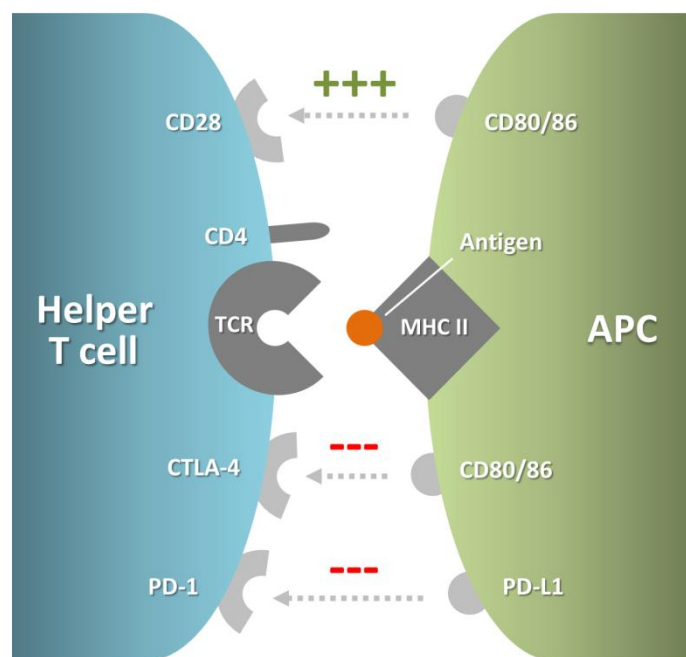


Fig. 1: Interaction between $CD4^+$ helper T cells and APCs.

Helper T cells require antigen presentation of professional APCs. Antigen is presented on the MHC class II and recognized by the TCR of $CD4^+$ T cells. Presence of coinhibitory and costimulatory molecules on APCs and T cells influence the efficacy of T-cell response: CD80 and CD86 expression on APCs can have a costimulatory or coinhibitory effect, dependent on the receptor they bind to on the T cell—CD28 as stimulator and CTLA-4 as inhibitor. PD-L1 is an effective inhibitor when binding to PD-1 receptor on T cells and is found to be overexpressed on many cancers. Figure shows simplified schematic illustration. CD = cluster of differentiation, TCR = T-cell receptor, CTLA-4 = cytotoxic T lymphocyte-associated antigen 4, PD-(L)1 = programmed death (ligand) 1, MHC = major histocompatibility complex, APC = antigen-presenting cell, DC = dendritic cell

case an additional second signal (CD80/86-CD28) is available. In 1989, Lurquin *et al.* published that T cells are generally capable of identifying tumor antigens (12). They found that CTLs were able to recognize a mutated self-peptide of P815 mastocytoma cancer cells in a murine model. They identified that the peptides had mostly a length of 8 to 10 amino acids, representing the proteins built within the cells. In the meantime, specific subsets of tumor antigens were discovered which can be distinguished depending on their specificity for tumor tissue:

1.1 Antigenes with low tumor specificity

Tumor-associated antigens (TAAs) are present on normal body tissue and cancer cells. They are either expressed to a higher amount on tumor cells such as human epidermal growth factor receptor 2 (HER2) in breast cancer (13) or vascular endothelial growth factor (VEGF) in renal cell carcinoma (14) or they are specific for the tissue from which the tumor originated (tissue differentiation antigens). A variety of targetable tissue differentiation antigens are known such as Tyrosinase (15), carcinoembryonic antigen (CEA) (16), Melan-A (MART-1) (17) or CD19. The latter is expressed on B cells and harnessed as target of CAR-modified T-cell therapy with high response rates (18, 19).

TAAs are found in the majority of individuals, which renders them applicable in immunotherapy for a large patient collective. On the other hand, since they are found on normal tissue, central tolerance can lead to decreased TCR-mediated responses. In addition to that, by targeting healthy cells, immunotherapy involving TAAs can lead to on-target off-tumor side effects (20), specified in 2.2.

1.2 Antigenes with high tumor specificity

Cancer-germline antigens (CGAs; also known as cancer-testis antigens) are expressed on germ cells and trophoblast tissue (21) but also on a variety of solid tumors including metastatic melanoma, lung and breast carcinoma (22). They contain the MAGE and BAGE family among others (23). Since they have not been presented in the thymus during central selection, no tolerance induction is expected. In addition, they are not expected in normal tissue and therefore allow strictly tumor-specific targeting (24). Using CGAs for TCR-mediated immunotherapy can nevertheless cause severe side effects in case cross-reactivity occurs (see 2.2).

Tumor-specific antigens (TSA) are exclusively expressed on tumor cells. When targeted, they are not expected to provoke autoimmunological effects nor does central tolerance play a role since they differ from antigens on healthy tissue (25). Some TSAs are shared among patients such as the BCR-ABL fusion protein in chronic myeloid leukemia or the mutated proto-oncogene product KRAS in several cancer entities (26). However, most of them are unique to each patient and need to be identified in individualized approaches, as was performed in the present study. A procedure referred to as “reverse immunology” is applied based upon the assumption that somatic mutations can predict those TSAs (27). Therefore, the genome of the tumor is sequenced and neoepitopes can be predicted *in silico*.

The amount of mutations in a tumor—potentially resulting in TSAs—is called mutational burden/load. It varies among tumor entities, essentially depending on the mutagens the tumors were exposed to. High mutation burdens can be found in melanoma, lung, stomach, colorectal, endometrial, and cervical cancers (28). Pediatric tumors such as medulloblastoma (MB) are known to have a very low mutational load and low immunogenicity (29). However, even tumors with low mutational loads can mount a relevant T-cell response: Tran *et al.* identified mutation-specific CD4⁺ cells in a patient with cholangiocarcinoma which contained only 26 mutations (30). In addition, Leisegang *et al.* showed that targeting only one mutation was sufficient for eradication of a solid tumor by T-cell therapy (27).

1.3 The concept of immunoediting

Although tumors can express (neo)antigens readily recognized by the immune system, they manage to evade the body's immune attack efforts. In 2007, Swann *et al.* observed that tumors expressing tumor-associated glycoprotein (Tag) are able to develop in immunocompetent mice despite Tag-specific immune responses (31). In another study, 9 out of 10 patients with metastatic gastrointestinal cancers generated T-cell responses against somatic mutations expressed by their tumors (32). Other studies proved the existence of mutation-reactive CD4⁺ cells in a patient with metastatic epithelial cancer originating from the bile ducts (30).

This paradoxical phenomenon of apparently unhindered cancer growth in a functional immune system is known as cancer immunoediting which is differentiated into the three phases elimination, equilibrium and escape (33):

1.3.1 Elimination

In the early 20th century, Paul Ehrlich postulated that the immune system is able to recognize and eliminate cancer cells (34, 35). Years later, Burnet and Thomas called this observation “immune surveillance” and described it as the continuous active effort of lymphocytes to detect and suppress carcinogenesis (36). In the elimination phase, the innate and adaptive immune systems manage to inhibit malignant growth. Several pro-inflammatory cytokines such as IL-12 and IFN- γ play a critical role in this phase (33). Natural killer (NK) cells-mediated killing of tumor cells initiates adaptive immune responses: NK cells promote the maturation of DCs and their migration to lymph nodes, which then prime T cells. The naïve T cells develop into CD8⁺ effector T cells that can now specifically target and kill tumor cells.

T cells are the strongest effectors of the immune system. Their enrichment in the tumor tissue—then referred to as tumor infiltrating lymphocytes (TILs)—is associated with a better prognosis of patients with melanoma (37) and other types of cancer, such as ovarian adenocarcinoma (38). In addition, the presence of NK cells in the tumor is correlated with a better patient survival for gastric carcinoma (39), squamous cell lung carcinoma (40) and colorectal cancer (41). Those cell entities induce cell apoptosis *via* the granule exocytosis pathway using perforin (pfp) or the Fas pathway (33). Mice lacking perforin were

more susceptible to lymphomas (42) as well as injected tumor cell lines (33). An important cytokine, regarding promotion of tumor cell recognition and elimination, is IFN- γ . It is released not only by NK cells but also by mature differentiated CD8⁺ T cells and some types of CD4⁺ T cells, together with TNF- α . By upregulating the expression of MHC class I and MHC class II molecules on tumor cells as well as tumor-resident APCs, both Th1 cytokines are able to enhance the immune response (43). IFN- γ -insensitive mice show increased tumor growth and frequency (44), especially when combined with deficiency of the p53 tumor-suppressor gene (45). In addition, mice deficient of both pfp and IFN- γ are significantly less capable of preventing metastasis as compared with mice either pfp-deficient or IFN- γ -deficient. The latter two are both comparable in terms of susceptibility to mice depleted of NK cells (46).

1.3.2 Equilibrium and escape

The equilibrium phase can last for years (47): Tumor cells become resistant to the immune attack, due to immune selection. In this process, growth of tumor variants which are more durable towards the immune system is encouraged and immunogenicity of the tumor is reduced.

During escape phase, the tumor starts to grow uncontrollably, achieving immunological tolerance. This is due to several mechanisms, affecting both effector and tumor cells:

On the effector side, TILs are known to be impaired: Due to loss of their signal transducer chain, which is part of the TCR-CD3 complex, T-cell activation upon antigen binding is compromised (48). Moreover, Strønen *et al.* tested the responsiveness of unaltered T cells from healthy donors towards melanoma-associated antigens from three melanoma patients (49). The donor-derived T cells were able to induce T-cell responses against 11 of 57 predicted HLA-A*02:01-binding epitopes as opposed to the autologous TILs which had mounted responses to only 2 of the 57 epitopes. This suggests that the neglect of tumor antigens by TILs can be bypassed by using an allogenic T-cell repertoire, as performed in this project.

On the other hand, the immunosuppressive tumor microenvironment plays an important role. Radoja *et al.* showed that impaired T-cell efficiency on the tumor site does not necessarily imply generally diminished T-cell function in a murine model (50). There are several cytokines, ligands and cell types involved in decreasing antitumor immunity: Programmed cell death 1 ligand 1 (PD-L1) is found on many cancer cells and inhibits tumor-specific T-cell response by binding its receptor programmed cell death protein 1 (PD-1) (51). PD-1 and cytotoxic T lymphocyte-associated antigen 4 (CTLA-4) are inhibitory immune checkpoints. They are physiologically located on T cells in order to prevent overactivation. In tumor escape, PD-1 is exploited by tumors to suppress T-cell response (52, 53). Tumors also intervene directly into apoptosis mechanisms: On the one hand, they evade elimination by overexpressing anti-apoptotic molecules (54). On the other, they are capable of inducing apoptosis in T cells by releasing pro-apoptotic vesicles (55). Finally, they secrete soluble factors such as VEGF, which impair the development of DCs, as well as anti-inflammatory mediators such as TGF- β and IL-10 in order to escape immune attack (56, 57). A further mechanism exerted by tumor tissue is down-regulation of MHC molecules to reduce

antigen-presentation (27, 58). An important role is also attributed to regulatory T cells (Tregs), usually responsible for suppression of immune responses to prevent autoimmunity. They have been shown to increase in number in the periphery during cancer progression, thus contributing to immune escape of the tumor (59).

2 Immunotherapy as a fourth pillar of cancer treatment

Cornerstones in cancer treatment have been surgery, chemotherapy and radiotherapy, often combined to improve clinical outcome. Recently, immunotherapy has gained in importance, enhancing the body's capacity of targeting malignant cells.

An early immunotherapeutic approach was performed by William B. Coley (60): In 1893, he observed cancer regression in a patient suffering from erysipelas. He assumed that this was due to bacteria and developed a mixture of killed bacteria, which was used to fight cancer for decades. However, today researchers attribute the tumor decrease to the intense immune response, triggered by the infection. In 1900, Paul Ehrlich developed the idea of "magic bullets", today known as antibodies, which could target receptors on cancer cells or pathogens specifically without harming healthy tissue (61).

Immune checkpoint inhibitors block molecules such as CTLA-4 and PD-1 and thereby lead to enhanced T-cell response due to decreased inhibition of T cells. They have been effective in several malignancies such as melanoma, non-small cell lung cancer, renal cell carcinoma and Hodgkin lymphoma (62, 63). However, experience in pediatric malignancies is limited: There are ongoing studies regarding Hodgkin's disease and non-Hodgkin's lymphoma and an upcoming trial concerning relapsed/refractory acute myeloid leukemia (64).

Another recent immunotherapeutic approach implies the engineering of bispecific antibodies that can link T cells and target cells by binding to both of them and thereby activating the T cell. Blinatumomab targets CD3 (T cells) and CD19 molecules (leukemic blasts) and is used successfully for treatment of chemotherapy-refractory ALL (65).

2.1 Peptide vaccination

Peptide vaccination is intended to induce immune response by administering tumor-specific peptides. Peptide vaccines generally have a favorable toxicity profile, they are effective and easy to synthesize (66). However, are prone to rapid degradation by peptidases (67) and they can lead to a functional deletion of tumor-specific CTLs and therefore immune tolerance (68), further discussed in D5. Slingluff *et al.* were able to induce helper T-cell responses in a high percentage of patients suffering from melanoma by injecting a vaccine composed of six melanoma-associated peptides (69). Schwartzentruber *et al.* compared treatment of advanced stage melanoma patients with IL-12 alone to treatment with IL-12 combined with a gp100 peptide vaccine (70). Patients treated with the vaccine showed significant improvement in clinical response and had a significantly longer progression-free survival. Another study

detected increase in disease-free survival in breast cancer patients upon treatment with E75 vaccine, which is derived from the HER2 protein (71). In addition to melanoma and breast cancer, cancer vaccines for several cancer entities have been included into clinical trials such as for lung cancer (72), pancreatic cancer (73), esophageal cancer (74), gastric cancer (75) and head and neck cancers (76).

2.2 Adoptive T-cell transfer

Adoptive T-cell transfer (ATT) launched a new era of immunotherapy, engaging the tumor cells specifically and effectively. In autologous ATT, endogenous T cells of the patients are extracted, expanded *in vitro* and finally administered back into the patient.

Starting in the late 1980ies, Rosenberg *et al.* extracted tumor tissue of melanoma patients, isolated the TILs, expanded them *ex vivo* and infused them back into the patients. The reimplanted TILs showed increased activity but were not very efficacious, as only in one of eleven patients a complete T-cell response could be observed (77). In 2002, their group successfully improved persistence of transferred T cells and therefore efficacy by lymphodepletion of the patients prior to T-cell transfer (78, 79). Multiple independent studies analyzing ATT in metastatic melanoma have reported 40 – 50 % objective responses and even 10 – 25 % complete remissions in treated patients (80). Moreover, Tran *et al.* showed that the patients with cholangiocarcinoma mentioned in 1.2 experienced objective regression of metastases and stabilization of disease after infusion of a highly enriched population of TILs, 25 % of which consisted of mutation-specific CD4⁺ T cells (30).

While ATT of TILs was very effective treating melanoma, TILs with antitumor reactivity are not present in many types of cancer (81). Regarding TILs derived from pediatric solid tumors, an early study examined osteosarcomas, Wilms' tumors, soft-tissue sarcomas and neuroblastomas (82): They were not able to identify TILs in most of the tumors nor could the TILs be expanded *ex vivo* sufficient for ATT. In order to enhance ATT efficacy, new strategies use genetically modified T cells either by implementing a TCR (83) or chimeric antigen receptor (CAR)(84), both capable of specifically targeting tumor antigens (Fig. 2). While ATT using engineered TCRs allows a highly specific immune attack, it also requires the identification, isolation and sequencing of tumor-specific TCRs. Tumor-specific TCRs are cloned and

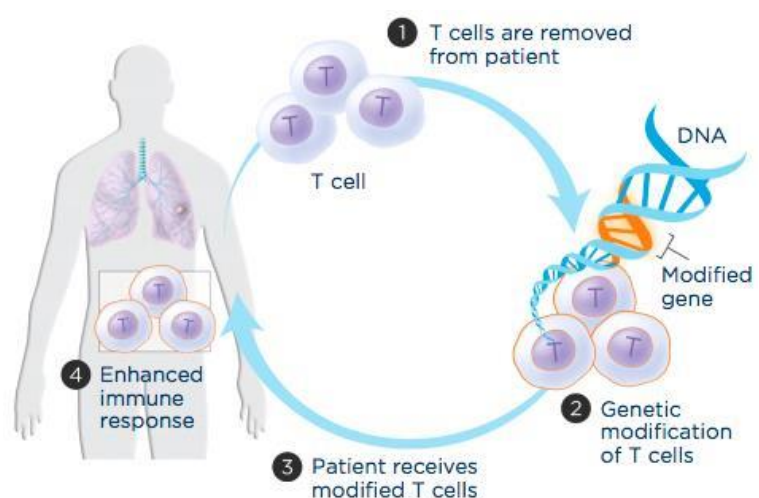


Fig. 2: Concept of adoptive T-cell transfer.

Patient's T cells are extracted, optionally modified genetically *in vitro*, expanded in number and infused back into the patient where they can enhance the immune response. Source: LUNGeivity Foundation (2016)

transduced into T cells *via* retro- or lentiviral vectors (85, 86). Moreover, those TCRs have to recognize not only the peptide but also the combination with the MHC to which it is bound. CARs on the other hand are fusion molecules consisting of an antibody's variable region bound to costimulatory and T-cell receptor subunits (CD3zeta). The CD3zeta and costimulatory domains allow T-cell activation and expansion upon antigen binding. CARs recognize their antigen in an MHC-independent manner (87), but are restricted to surface antigens. CD19-directed CAR T-cell therapy has proven to be very effective in relapsed/refractory B-cell acute lymphoblastic leukemia (ALL) and chronic lymphocytic leukemia (CLL) (88, 89). In general, ATT has mediated considerable cancer regression in melanoma, cervical cancer, lymphoma, leukemia, bile duct cancer and neuroblastoma (79).

However, there have been drawbacks in adoptive T-cell therapy due to TCR-mediated side effects which are classified into on-target/off-tumor and off-target/off-tumor side effects (90) and are both able to cause healthy tissue damage. In 2009, 36 patients were treated with TCR-transduced T cells targeting melanoma differentiation antigens Melan-A (MART-1) or gp100. A third of the patients showed cancer regression but half of the patients developed not only vitiligo but sometimes also destruction of melanocytes in the eye and the inner ear (on-target/off-tumor) (91). In a trial realized in 2013, myeloma and melanoma patients were treated with T cells engineered to express a MAGE-specific TCR. Due to cross-recognition of a similar peptide derived from the muscle protein Titin, the treatment led to fatal toxicity against cardiac tissue (92, 93). In an additional trial using TCRs against MAGE-derived epitopes, severe damage to the brain tissue was observed, leading to coma and death in several patients. This occurred as the TCR recognized a different but related epitope expressed at very low levels in the brain (94). Both examples constitute off-target/off-tumor side effects. Targeting neoepitopes derived from TSAs, as performed in this study, can help reduce toxicity from such off-tumor effects.

3 Medulloblastoma, the most common malignant brain tumor in childhood

Tumors of the central nervous system (CNS) account for about a fifth of childhood tumors and constitute the leading cause of cancer-related death in children (Fig. 3) (95, 96). Among malignant tumors of the CNS, MB is the most frequent one, located in the cerebellum. It is an aggressive, fast-growing, highly malignant cancer, classified as WHO grade IV. It mainly affects children between five and nine years, but can also develop in infants as well as adults, although rarely after the fourth decade of life (97).

Primary symptoms in patients with MB are due to increased intracranial pressure, resulting in head ache, impaired vision, morning vomiting and altered mental status (98). Local damage of cerebellar structures manifests with ataxia, dizziness and general impairment of motor function. Secondary affected brain structures as well as frequently occurring metastases can imply further neurological deficits.

3.1 Classification and pathogenesis

Recently, MB has been classified into four subgroups based on histology and molecular features (99), with a focus on molecular pathways (100). The subgroups comprise the Wnt group, the sonic hedgehog (SHH) group, as well as Group 3 and Group 4. In the latter three, MB arises from cerebellar progenitor cells. Underlying mutations either enhance the SHH pathway (SHH group) or include amplification of MYC or MYCN genes among others (Group 3 and 4) (101). Wnt-associated MBs, however, imply the Wnt pathway and arise from the lower rhombic lip. They are attributed the best prognosis whereas group-3 MB patients have the worst outcome (102).

In terms of histology, several subtypes are distinguished: classic, large cell/anaplastic (LCA), nodular/desmoplastic and MB with extensive nodularity (103). Among these, LCAs have the worst prognosis while nodular/desmoplastic histology has rather favorable outcomes.

Although some mechanisms leading to development of MB are known, it generally remains a cancer with a heterogeneous origin. Like other pediatric tumors, it has a low somatic mutation burden compared to other solid tumors (104). Next-generation whole genome and exome sequencing have recently increased knowledge about genetic underlying aberrations. In three independent studies from 2012, the average number of somatic, non-silent mutations—single nucleotide variants (SNVs) and indels—per MB genome ranged from only ten to twelve (104-106). There was a positive correlation between patient age and mutation rate, implying that adult MBs harbor considerably more mutations. Genetic heterogeneity underlying MB was underscored by the fact that among all 2,102 mutated genes identified in the three studies there were only 12 genes recurrently mutated (107).

Another large study of the genomic landscape of MB was recently performed by Northcott *et al.* who included whole genome and exome data of almost 500 untreated MB patients, ranging from 1 month to 50 years (108). They discovered a median of 698 mutations. Driver mutations in the coding regions were located in genes PTCH1, DDX3X, KMT2D and others which were assigned to patients belonging to Group 3 and Group 4. In Wnt-driven and SHH-driven MB, driver mutations were found in the genes of respective

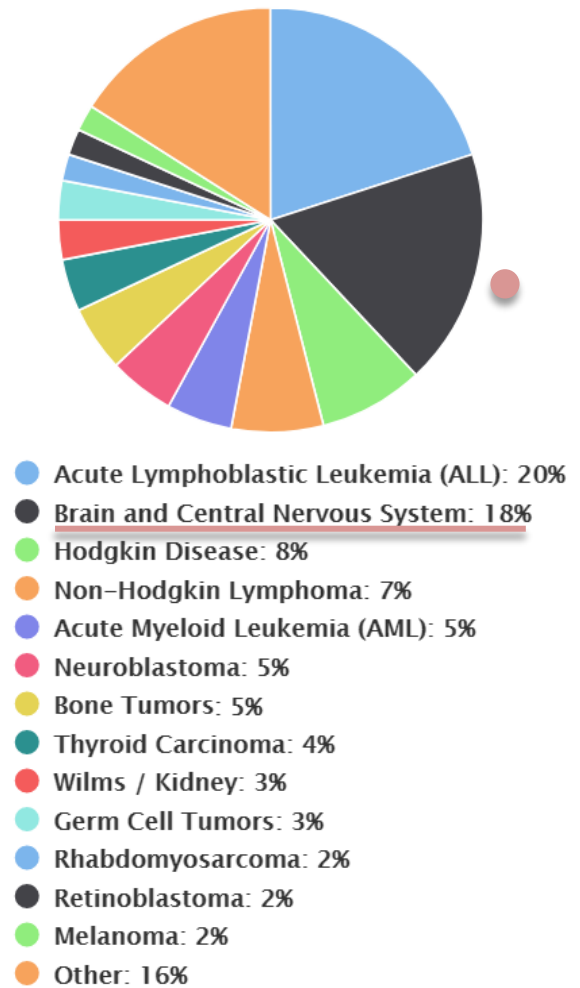


Fig. 3: Distribution of childhood cancer diagnoses per year.

Tumors of the CNS, including medulloblastoma, account for about a fifth of childhood malignancies. Chart comprises patients aged 0 – 19. Source: American Cancer Society, Cancer Facts and Figures (2014)

pathways. Another reported gene found mutated in MB is the well-known tumor suppressor gene *TP53*. In contrast to these mutations associated with a proven impact on tumorigenesis of MB, Northcott *et al.* reported a great number of low-frequency gene alterations which are not yet examined, but with possibly crucial roles.

3.2 Therapy

Treatment of MB has improved significantly and combines surgical resection, chemotherapy and irradiation (109). Approximately 80 – 85 % of average-risk patients and up to 70 % of high-risk patients can be cured of their disease, depending on subgroups (110). However, persistent adverse effects of these multi-approach treatment regimens include developmental, neurological, neuroendocrine and psychosocial deficits (111). Especially very young patients are susceptible to irradiation which makes it necessary to carefully evaluate the involved benefit and potential damage. Moreover, relapse of MB, which occurs in 20 – 30 % (112), remains a major problem: It has presented altered biology resulting in a more aggressive, uncontrollable growth (113). In a retrospective study including 55 MB patients, they reported a median survival after relapse of less than a year and a 3-year survival of 18 % (114).

4 Objective: Inducing a *de novo* immune response against tumor-derived peptides

The goal of this project was to determine whether tumor-specific neoepitopes derived from variants of two MB patients prove to be immunogenic. Reverse immunology approach was applied to find patient-specific neoepitopes: Tumor-specific non-synonymous mutations were identified by whole exome sequencing and confirmed by deep sequencing. MHC binding affinity to patients' HLA types was predicted *in silico* and binding peptides were synthesized for immunogenicity testing. Blood cells from healthy donors provided DCs for antigen presentation of peptides to donor-derived autologous T cells. In case that the peptide/HLA combination was recognized by the T cells, a *de novo* T-cell response was induced. Memory cells were developed ensuring a quick reinitiation of response upon further antigen exposure. Eventually, after seven restimulations with antigen presentation, the epitope was added again to reinduce the T-cell response which was then measured and quantified by IFN- γ and TNF- α release.

In this “proof of principle” experiment we investigate T-cell responses against neoantigens which could then have several implications: First, we want to prove that medulloblastoma potentially harbors neoepitopes capable of inducing an immune response. We want to confirm that unaltered third-party T cells are capable of recognizing tumor epitopes neglected by the patient's endogenous TILs. Second, further investigations can identify the TCRs involved in positive T-cell responses, determine their sequences and synthesize them. Approaches such as TCR-transduced ATT or peptide vaccination using a patient-adjusted peptide cocktail could allow a completely individualized treatment, especially for advanced tumor patients, and thus create new therapeutic possibilities.

B Materials and Methods

1 Materials

1.1 Equipment and software

Autoclaves	VX-150 and DX-65, Systec, Linden, Germany
Cell counting auxiliaries	Cell Counting Chamber Neubauer, Chamber Depth 0.1 mm, Paul Marienfeld, Lauda-Königshofen, Germany
Centrifuges	Multifuge X3R and Mini Centrifuge Fresco 17, Heraeus, Hanau, Germany Centrifuge 5810 R, Eppendorf, Hamburg, Germany
Cooling units	FD 7202, Bosch, Munich, Germany Freezer (-20 °C) Premium No Frost, Liebherr, Biberach an der Riß, Germany Freezer (-86 °C) HERAFreeze HFU T Serie, Heraeus, Hanau, Germany Cryogenic Freezer MVE 600 Serie, Chart, Luxemburg
Flow cytometer	BD LSRFortessa Cell Analyzer, BD, Franklin Lakes, USA
Freezing container	Nalgene Mr. Frosty, Thermo Fisher Scientific, Waltham, USA
Gamma irradiation devices	Biobeam 8000, Gamma-Service Medical GmbH, Leipzig, Germany
Incubator	HERAcell 240 CO ₂ Incubator, Thermo Fisher, Waltham, USA
Laminar flow hood	Herasafe HS 12, Heraeus, Hanau, Germany
Microscopes	Leica DM IL, Leica, Wetzlar, Germany
Pipettes (electrical)	Easypet 3, Easypet Original, Eppendorf, Hamburg, Germany
Pipettes (manual)	2.5 µl, 20 µl, 200 µl, 1000 µl Eppendorf Research, Eppendorf, Hamburg, Germany
Software	BD FACSDiva 8.0.1, BD Biosciences, Franklin Lakes, USA FlowJo 10.0.7r2, Ashland, USA GraphPad PRISM 7.0, La Jolla, USA Microsoft Office 2010, Redmond, USA
Vacuum pump	Vakuumsystem BVC 21 NT, Vacuubrand, Wertheim, Germany
Test tube shaker	Vortex Genie 3, IKA-Werke, Staufen, Germany
Water bath	3043, Köttermann, Uetze/Hänigsen, Germany

1.2 Solutions, media and sera for cell culture

Albiomin 5 % infusion solution human albumin (HSA)	Biotest, Dreieich, Germany
CliniMACS PBS/EDTA buffer	Miltenyi Biotec, Bergisch Gladbach, Germany
Biocoll separating solution	Biochrom, Berlin, Germany
Brefeldin A	Sigma-Aldrich, Steinheim, Germany
Compensation beads	CompBeads Compensation Particles Set, BD Biosciences, San Diego, USA
DMSO	Honeywell, Seelze, Germany

Dulbeccos phosphate buffer saline (PBS)	Gibco, Life Technologies, Darmstadt, Germany
FACS clean/rinse/flow	BD, Erembodegem, Belgium
Fix & Perm cell permeabilization kit	Life Technologies, Frederick, USA
GM-CSF	Sanofi, Bridgewater, USA
HEPES buffer 1 M	Biochrom, Berlin, Germany
Human AB serum	Human AB serum was kindly provided by Prof. R. Lotfi, University Hospital Ulm, Institute for Transfusion Medicine and German Red Cross Blood Services Baden-Württemberg—Hessen, Institute for Clinical Transfusion Medicine and Immunogenetics, both from Ulm, Germany
IL-1 β , IL-4, IL-6, IL-7, IL-15, TNF- α	CellGro Preclinical Recombinant Human Cytokines, CellGenix, Freiburg, Germany
Ionomycin	Merck, Darmstadt, Germany
L-Glutamine 200 mM	Biochrom, Berlin, Germany
Paraformaldehyde (PFA) 4 %, in PBS, pH 7.4	Morphisto GmbH, Frankfurt am Main, Germany
PGE2	Sigma-Aldrich, Steinheim, Germany
Phorbol 12-myristate 13-acetate (PMA)	Merck, Darmstadt, Germany
Trypan blue	Gibco, Life Technologies, Darmstadt, Germany
VLE RPMI 1640 medium	Biochrom, Berlin, Germany

1.3 Buffers and cell culture medium

DC medium	VLE RPMI 1640 Medium + 10 % human AB serum + 1 % HEPES Buffer 1 M + 1 % L-Glutamine 200 mM
Freezing medium	Human serum albumin (Albiomin 5 % infusion solution) + 10 % DMSO
Staining buffer	CliniMACS PBS/EDTA Buffer + 10 % Human serum albumin (Albiomin 5 % infusion solution; end concentration 0.5 % albumin)

1.4 Consumables

Blood collection tubes	S-Monovette 9ml K3E, Sarstedt, Nümbrecht, Germany
Cell culture flasks with ventilation caps	25 cm ² , 75 cm ² , 175 cm ² , Sarstedt, Nümbrecht, Germany
Cell culture multiwell plates, 6 well	Costar Corning Incorporated, New York, USA
Cell culture multiwell plates, 48 well	Cellstar Greiner Labortechnik, Kremsmünste, Austria
Cell culture multiwell plates, 96 well	Nunclon Delta Surface, Thermo Fisher Scientific, Waltham, USA

Compresses	Gauze Compresses 10 x 10 cm, Nobamed Paul Danz, Wetter, Germany
Cover slips	Menzel-Gläser 20 x 20 mm, Gerhard Menzel, Braunschweig, Germany
Freezing tubes	Cryo Pure Gefäß 1.8 ml, Sarstedt, Nümbrecht, Germany
Pasteur pipettes	Glass Pasteur Pipettes 230 mm, Brand, Wertheim, Germany
Pipette tips	0.1 - 2.5 µl, 10 µl, 20 µl, 100 µl, 2 - 200 µl, 1000 µl, Sarstedt, Nümbrecht, Germany
Reaction vessels	15 ml, 50 ml Falcon, Corning Science, Tamaulipas, Mexico 15 ml, Sarstedt, Nümbrecht, Germany 50 ml, Orange Scientific, Braine-l'Alleud, Belgium 1.5 ml, 2 ml, Eppendorf Safe Lock Tubes, Eppendorf, Hamburg, Germany
Round bottom tubes with cell strainer snap cap	5 ml Polystyrene Round Bottom Tube, Falcon, Corning Science, Tamaulipas, Mexico
Safety gloves	Vaso Nitril Blue, B. Braun Melsungen, Melsungen, Germany
Serological pipettes	2 ml, 25 ml, Costar Stripette, Corning Incorporated, New York, USA 5 ml, 10 ml, Serological Pipette, Sarstedt, Nümbrecht, Germany
Skin disinfectant	Cutasept F and Sterilium Classic Pure, Bode Chemie, Hamburg, Germany
Surface disinfectant	Ethanol 80 % MEK/Bitrex, CLN, Niederhummel, Germany Bacillol AF, Paul Harmann, Heidenheim, Germany

1.5 Antibodies

Fluorochrome	Antigen	Clone	Manufacturer
APC	CD8	SK1	BD Biosciences, Franklin Lakes, USA
APC	CD80	2D10	Biolegend, San Diego, USA
eFluor 780	Fixable viability dye		eBioscience, ThermoFisher, Waltham, USA
BB515	CD62L	DREG-56	BD Biosciences, Franklin Lakes, USA
BUV395	CD3	SK7	BD Biosciences, Franklin Lakes, USA
BV650	CD4	SK3	BD Biosciences, Franklin Lakes, USA
BV650	CD86	IT2.2	Biolegend, San Diego, USA
FITC	Lineage (CD3, CD14, CD19, CD20, CD56)	UCHT1, HCD14, HIB19, 2H7, HCD56	Biolegend, San Diego, USA
PacificBlue	TNF-A	MAB11	Biolegend, San Diego, USA
PE	CD83	HB15e	Biolegend, San Diego, USA
PE	IFN-γ	25723.11	BD Biosciences, Franklin Lakes, USA
PE-Cy7	CD45RO	UCHL1	Biolegend, San Diego, USA
PerCP	HLA-DR	L243	Biolegend, San Diego, USA

2 Methods

2.1 Induction of a mutation-specific *de novo* immune response

Each experiment began with the generation of dendritic cells (DCs) and peripheral blood lymphocytes (PBLs), included seven cycles of weekly PBL restimulation and finally concluded with a cytokine release assay of the stimulated cells (Fig. 4). The whole protocol took 10 weeks and was performed for 18 different donors. It was kindly provided by Armin Rabsteyn (University Hospital Tübingen / DKFZ Heidelberg) and Prof. Dr. Peter Lang (University Hospital Tübingen, General Pediatrics, Hematology/Oncology).

2.1.1 Generation of DCs and PBLs

All healthy blood donors gave written informed consent prior to blood sampling. Blood samples were obtained either by venous puncture of 60 – 90 ml EDTA blood or derived from buffy coats kindly provided by Prof. Ramin Lotfi (University Hospital Ulm, Institute for Transfusion Medicine and German Red Cross Blood Services Baden-Württemberg—Hessen, Institute for Clinical Transfusion Medicine and Immunogenetics, Ulm, Germany).

On day 1, peripheral blood mononuclear cells (PBMCs) were isolated from blood samples *via* Biocoll

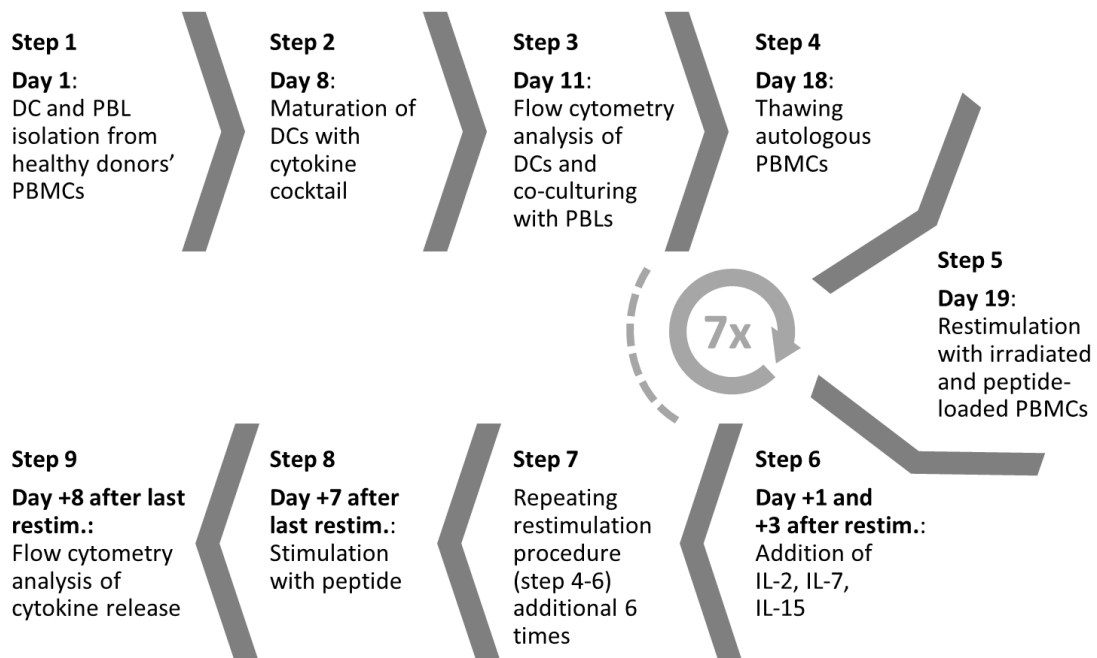


Fig. 4: Experimental design: Induction of neoantigen-specific *de novo* T-cell responses.

On day 1, monocytes/DCs and PBLs were extracted from healthy donors' PBMCs. Maturation cocktail was added to the DC culture on day 8. DC maturity was proved 3 days later *via* flow cytometry and donors' PBLs were cocultured with the mature DCs loaded with tumor-specific peptide. In a cycle of 7 weekly restimulations, freshly thawed autologous PBMCs were loaded with peptide, irradiated and added to the culture in order to restimulate the T cells. Cytokines were added on day +1 and +3 after restimulation. On day +7 after last restimulation, T cells were stimulated and T-cell responses were measured 14 hours later by assessing IFN- γ and TNF- α secretion *via* flow cytometry. DC = dendritic cell, PBL = peripheral blood lymphocyte, PBMC = peripheral blood mononuclear cell

density gradient centrifugation:

The blood sample was diluted 1:2 to 1:4 with phosphate buffered saline (PBS). 35 ml of the diluted sample was cautiously layered on 15 ml Biocoll and centrifuged at 800 rcf for 30 minutes without brake. The buffy coat was aspirated, washed twice with PBS (500 rcf for 10 minutes, then 250 rcf for 10 minutes) and resuspended in DC medium. Cell number and cell viability were assessed (see 2.3.1) and half of the cells were frozen for weekly restimulations. The other half was cultured in DC medium at a concentration of 5×10^6 /ml and incubated in culture flasks (75 cm² when volume \leq 15 ml, 175 cm² when volume 15 – 35 ml). After 2 hours, non-adherent cells (PBLs) were centrifuged at 400 rcf for 10 minutes and resuspended in DC medium containing 5 ng/ml IL-7. The adherent fraction (monocytes, DCs) was washed three times by carefully rinsing with PBS. Fresh DC medium supplemented with IL-4 (40 ng/ml) and GM-CSF (100 ng/ml) was added to the adherent cells. Both PBLs and DCs were cultured for 7 days.

On day 8, DCs were centrifuged at 400 rcf for 6 minutes and resuspended in fresh medium containing IL-1 β (10 ng/ml), IL-4 (40 ng/ml), IL-6 (10 ng/ml), GM-CSF (100 ng/ml), TNF- α (10 ng/ml) and PGE₂ (1000 ng/ml).

2.1.2 Harvest of DCs, peptide loading and coculture of DCs and PBLs

On day 11, mature DCs were harvested by tapping the flask and rinsing it with PBS twice and carefully in order not to remove adherent immature cells. 2×10^6 cells were taken for flow-cytometric analysis of DC maturity (see 2.1.3). Mature DCs were loaded with tumor-specific peptides and cocultured with PBLs:

Peptides derived from tumor-specific mutations were identified as described in C1. Lyophilized peptides were diluted in dimethyl sulfoxide (DMSO) at a stock concentration of 10 mg/ml and further diluted with sterile H₂O to a concentration of 1 mg/ml. For each condition, mature DCs were transferred to a separate 15-ml tube, centrifuged at 400 rcf for 6 minutes and resuspended in 1000 μ l DC medium. Peptide was added at a concentration of 10 μ g/ml and incubated for 2 hours at 37 °C. Memory-cell controls were included by incubating DCs with diluted DMSO

Table 1: Antibodies for different staining conditions in DC maturity proof.

An isotype control was added to rule out unspecific binding of antibodies. An FMO control for PE CD83 was added for better assessment of its influence on measurement. DC = dendritic cell, FMO = fluorescence minus one

Isotype control	Staining buffer	42 μ l
	FITC Mouse IgG1, κ	2.5 μ l
	FITC Mouse IgG2b, κ	2.5 μ l
	PE Mouse IgG1, κ	1 μ l
	APC Mouse IgG1, κ	0.5 μ l
	BV650 Mouse IgG2b, κ	0.5 μ l
	PerCP Mouse IgG2a, κ	1 μ l
Stained	Staining buffer	34.5 μ l
	FITC Anti-Human Lineage Cocktail (CD3/14/19/20/56)	10 μ l
	PE Anti-Human CD83	1 μ l
	APC Anti-Human CD80	0.5 μ l
	BV650 Anti-Human CD86	0.5 μ l
	PerCP Anti-Human HLA-DR	1 μ l
	eFluor 780 Fixable Viability Dye (1:10 predilution)	2.5 μ l
FMO CD83	Staining buffer	35.5 μ l
	Antibodies as in "stained" condition but without PE Anti-Human CD83	

(final dilution 1:1000 according to DMSO dilution in peptides) and were treated similarly. Memory-cell controls were added in order to reveal already pre-existing memory-cell responses on final intracellular cytokine staining (ICS) which were not induced by DC-mediated antigen presentation.

PBLs were centrifuged at 300 rcf for 10 minutes and resuspended in DC medium at a concentration of 5×10^6 /ml.

After incubation with either peptide or memory-cell control, DCs were diluted with DC medium to a concentration of 0.5×10^6 /ml. One ml of both DC and PBL suspension was pipetted into one well of a 24-well plate and cocultured at 37 °C.

2.1.3 Maturity proof of DCs

DCs harvested on day 11 (see 2.1.2) were centrifuged at 400 rcf for 6 minutes and counted. 5×10^5 DCs were needed per stain, thus 2×10^6 for conditions “unstained”, “isotype control”, “stained” and “FMO CD83”. Isotype control was inserted to exclude unspecific binding. FMO CD83 was used since the CD83 antigen is considered the most important maturity marker of dendritic cells.

To block unspecific binding, those cells taken for staining were resuspended in CliniMACS buffer and 10 % human AB Serum at a concentration of 2×10^6 /ml and incubated on ice for 30 minutes. After washing at 450 rcf for 4 minutes, 5×10^5 DCs were diluted in a total volume of 50 μ l for each condition, with the amounts of staining buffer/antibody depicted in Table 1. After 10 minutes of staining at 4 °C, DCs were washed twice with staining buffer at 450 rcf for 4 minutes and measured on a BD LSRFortessa Cell Analyzer.

All antibodies were titrated beforehand to determine required concentrations. FITC anti-human lineage cocktail antibody consisting of CD3, CD14, CD19, CD20 and CD56 was used to exclude T cells, monocytes, macrophages, B cells and NK cells.

2.1.4 Weekly restimulations with autologous peptide-loaded PBMCs

Restimulations were performed on day +8, +15, +22, +29, +36, +43 and +50 after coculture. For restimulation, autologous PBMCs were used which have been frozen on day 1. Cells were thawed (see 2.3.2). The pellet was resuspended in 10 ml DC medium and rested overnight in a 25 cm² flask. Approx. 20 hours later, PBMCs were loaded with peptide: For each condition, PBMCs were transferred to a 15-ml tube, centrifuged at 300 rcf for 10 minutes and resuspended in 1000 μ l DC medium. Peptide at a concentration of 10 μ g/ml and diluted DMSO (final dilution 1:1000 according to DMSO dilution in peptides) were added to respective tubes. Tubes were incubated for 2 hours at 37 °C and then gamma-irradiated with 30 Gray in order to prevent cell culture growth. After irradiation, the cell suspension was diluted with DC medium to a concentration of 1×10^6 cells/ml. One ml supernatant was removed from each well of corresponding DC/PBL coculture plates and filled up with 1 ml peptide-loaded, irradiated autologous PBMCs.

One and three days after restimulation, 50 U/ml IL-2 and 10 ng/ml of each IL-7 and IL-15 were added. Three days after last (7th) restimulation, no cytokines were added in order not to influence flow-cytometric measurements the following week.

2.1.5 Quantification of IFN- γ and TNF- α release *via* flow cytometry

After 7 restimulations, T cells were stimulated with tumor-specific peptide and T-cell response was analyzed 14 hours later by ICS. Fig. 5 represents different conditions: Peptides that were applied to DC/PBL/PBMC cocultures during weeks of restimulations (column: peptide), stimulation solutions applied 14 hours prior to final ICS (column: simulation condition) and stains included in final ICS (column: staining condition).

Each well of 24-well plates was resuspended and 200 μ l cell suspension was transferred to a 96-well round bottom plate. After centrifugation at 300 rcf for 2 minutes, 100 μ l supernatant was removed from each well and replaced by 50 μ l of diluted Brefeldin A solution (end concentration 10 μ g/ml) and 50 μ l stimulation solution. Stimulation solution consisted of either the positive control containing phorbol-12-myristate-13-acetate (PMA) and Ionomycin (final concentration 50 ng/ml and 750 ng/ml, respectively), the tumor-specific peptide (final concentration 1 μ g/ml) or the negative DMSO control (final dilution 1:10000 in analogy to the diluted peptides). The latter served as basis for determining the fold change (FC), described in 2.2.

After 14 hours of incubation at 37 °C, ICS was performed: Cells were transferred to 1.5 ml Eppendorf tubes, washed twice at 450 rcf for 4 minutes and resuspended in 100 μ l staining buffer containing the extracellular staining antibodies indicated in Table 2. The solution was incubated for 15 minutes at room temperature (RT). 50 μ l Fixation Reagent was added to tubes and incubated for 15 minutes at RT. Cells

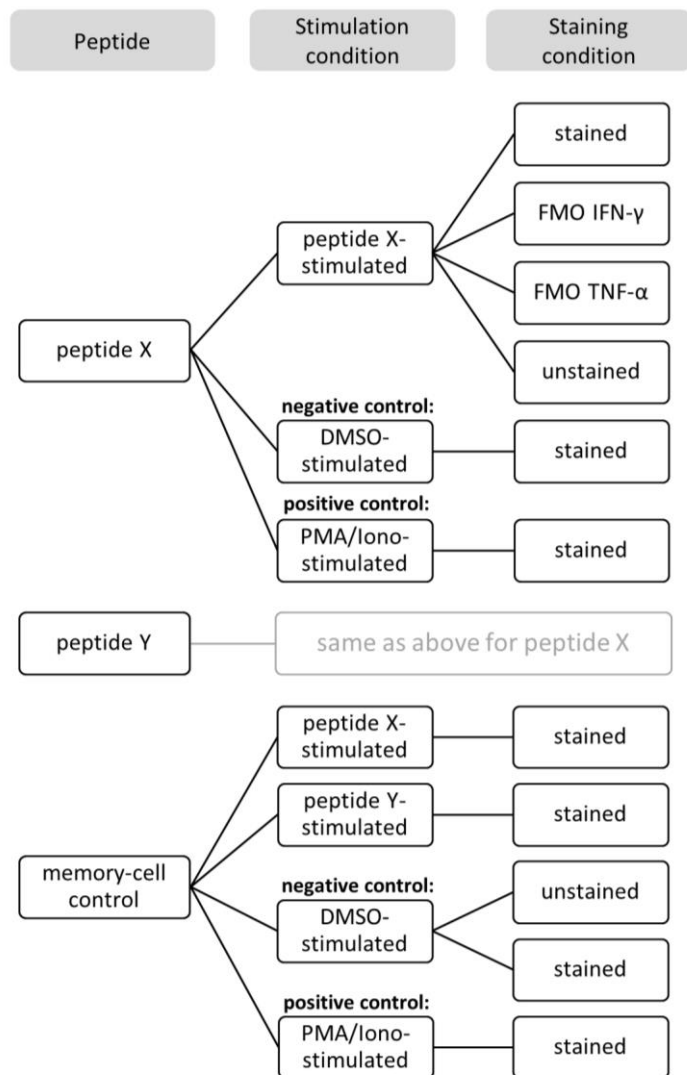


Fig. 5: Conditions of ICS panel.

For final ICS, cells that had been stimulated with different peptides and cells from memory-cell control were used for stimulation conditions: Apart from peptide stimulation there was a positive PMA/Iono control as well as a negative DMSO control. Peptides X and Y stand for arbitrary peptides. FMO = fluorescence minus one, DMSO = dimethyl sulfoxide, PMA = phorbol-12-myristate-13-acetate, Iono = Ionomycin, ICS = intracellular cytokine staining

were washed at 450 rcf for 4 minutes and pellets were resuspended in 50 μ l Permeabilization Reagent and the intracellular staining antibodies described in Table 2. Tubes were incubated for 30 minutes at RT, then washed at 450 rcf for 4 minutes, resuspended in 500 μ l staining buffer and measured on a BD LSRFortessa Cell Analyzer.

2.2 Determination of positive T-cell responses

To examine if mutation-specific peptides are capable of inducing T-cell responses, IFN- γ and TNF- α secretion values of both T-cell groups were required, one being the peptide-stimulated (sample) and the other the DMSO-stimulated (control) with stimulation taking place 14 hours prior to ICS. However, each corresponding pair belonging to those two T-cell groups had been treated equally during weeks of 7 restimulations, namely with peptide (for determination of *de novo* T-cell responses) or with DMSO (for memory-cell control). Determined values were put into relation to generate the FC. A FC of 1 means that control and sample showed the same amount of cytokine release. Whenever the IFN- γ and TNF- α release FC of a specific peptide exceeded 2, this particular peptide was considered positive in terms of T-cell response.

2.3 General cell culture

Cells were cultured at 37 °C with 5 % CO₂. Culture media are indicated in 1.3.

2.3.1 Counting cells

Depending on expected cell number, cells were diluted with PBS and then mixed with trypan blue 1:2. The suspension was transferred to a Neubauer counting chamber and assessed under the light microscope. As trypan blue only stains dead or defect cells, viable cells can be identified in four squares of the chamber. Cell concentrations were calculated using the following formula: (determined cell count average) x (dilution factor) x 10⁴ = cells/ml.

2.3.2 Freezing and thawing cells

For freezing, cells were resuspended in pre-cooled human serum albumin (HSA) supplemented with 10 % DMSO at a concentration of up to 6 x 10⁷ cells/1.8 ml and frozen in a freezing container (cooling rate

Table 2: Antibodies for ICS conditions.

First, extracellular stain antibodies were added to cells. After application of cell fixation and permeabilization reagent, intracellular stain antibodies were applied. FMO controls were included. FMO = fluorescence minus one, ICS = intracellular cytokine staining

	Extracellular stains	
Stained + FMO IFN-γ + FMO TNF-α	Staining buffer	86.5 μ l
	BB515 Mouse Anti-Human CD62L	2 μ l
	PE/Cy7 Anti-Human CD45RO	3 μ l
	eFluor 780 Fixable Viability Dye (not prediluted)	0.5 μ l
	APC Mouse Anti-Human CD8	5 μ l
	BV650 Mouse Anti-Human CD4	1 μ l
	BUV395 Mouse Anti-Human CD3	2 μ l
	Intracellular stains	
Stained	PE Mouse Anti-Human IFN- γ	20 μ l
	Pacific Blue Anti-Human TNF- α	1 μ l
FMO IFN-γ	Pacific Blue Anti-Human TNF- α	1 μ l
FMO TNF-α	PE Mouse Anti-Human IFN- γ	20 μ l

1 °C/minute). Vials were transferred to liquid nitrogen cryogenic freezers 24 to 72 h later. When thawing cells, they were rapidly warmed up to 37 °C in the water bath and resuspended in warm DC medium. They were washed twice at 300 rcf for 10 minutes.

2.4 Prediction of HLA binding affinity

In silico databases netMHCpan-2.4 and netMHC-3.0 (115) were consulted to predict binding affinity between MHC molecules and potential neoepitopes (mutant peptides). Peptides with a netMHC affinity score ≤ 500 nM (corresponds to a logscore of ≥ 0.426) were regarded as binders. Whenever a mutant peptide was predicted to bind an HLA type according to the databases while the corresponding wild-type peptide did not, the mutant peptide was synthesized and used for the project.

2.5 Statistics

Unpaired (Student's) t-test was applied to examine statistical difference when comparing means of two groups. It was performed with GraphPad PRISM 7.0. Significance level was set to a p-value of 0.05; designating $p < 0.05$ (*) significant, $p < 0.01$ very significant (**) and $p < 0.0001$ (****) extremely significant.

C Results

1 Preliminary work: Selection and generation of tumor-specific peptides derived from medulloblastoma

The preliminary work for this thesis contained recruitment of tumor samples from two MB patients (Prof. Martin Schuhmann, University Clinic Tübingen), identification of neoepitopes by sequencing (Christopher Schroeder, Nicolas Casadei and Sven Poths, Institute of Medical Genetics und Applied Genomics, Tübingen), binding affinity prediction (Christopher Mohr, Applied Bioinformatics Group, Tübingen) and peptide synthesis (Prof. Stefan Stevanović, Department of Immunology at Interfaculty Institute for Cell Biology, Tübingen) (Fig. 6).

1.1 Patients' characteristics

The two patients analyzed for this thesis were a female infant (patient 1) and a male juvenile (patient 2),

Table 3: Characteristics of two pediatric medulloblastoma patients.

In order to manufacture tumor-specific peptides, neoepitopes had to be detected, originating from tumor tissue, which was extracted from two patients with medulloblastoma. Adapted from Blaeschke, Paul *et al.* (2019)

	Patient 1	Patient 2
Sex	female	male
Diagnosis	medulloblastoma with extensive nodularity	anaplastic medulloblastoma
Location of primary tumor	infratentorial, infiltration of vermis	infratentorial, infiltration of cisterna ambiens
Initial diagnosis	Aug 2012	Jan 2014
Age when diagnosed	11 months	13 years, 8 months
Resection of primary tumor	Dec 2012	Jan 2014
Radio-/ chemotherapy	neo-adjuvant chemotherapy beginning in Aug 2012, then continued uninterruptedly until Aug 2014	chemotherapy from Mar 2014 to Apr 2015 / cranial radiation from Sept to Oct 2014
Metastasis/ relapse/ outcome	relapse in Apr 2014 with meningeal tumor spreading	primary metastasis on right temporal side / relapse in July 2015 / decease in Sep 2015
Tumor material used for project	from advanced biopsy performed in Aug 2012	from resection performed in Jan 2014
PBMCs used for project	from blood sample taken in Dec 2012	from blood sample taken in Jan 2014

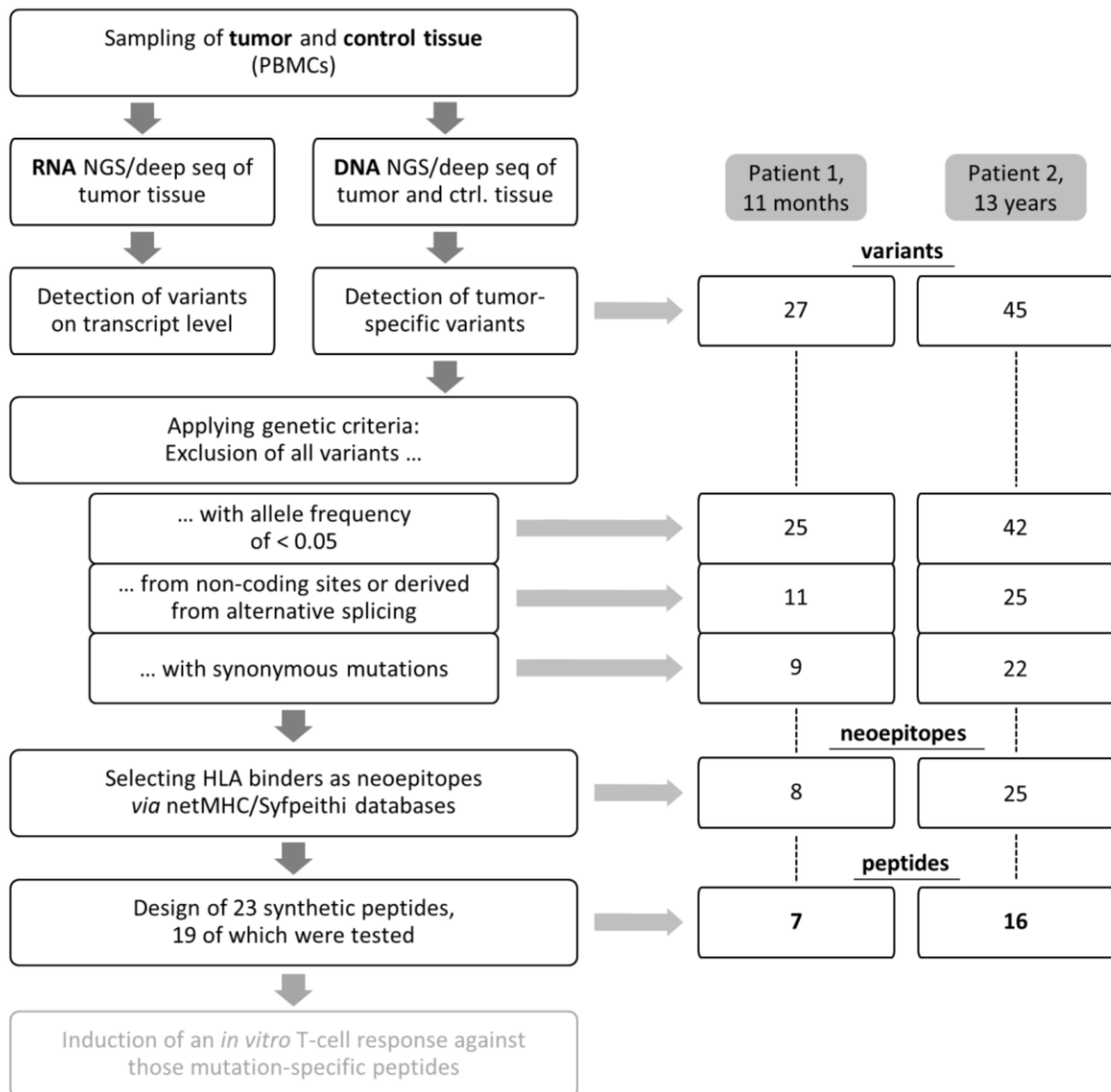


Fig. 6: Workflow: Algorithm for identification of tumor-specific neoantigens.

Whole-exome NGS was performed to identify tumor-specific mutations. Variants were further analyzed on transcript level by RNA NGS. The variants were now filtered by excluding non-detectable (AF < 5 % and/or depth < 20 reads), non-coding, synonymous mutations as well as weak HLA binders according to *in silico* prediction database netMHC. The boxes on the right side show how initial amount of patients' variants was reduced accordingly. The 23 final peptides then result from only 15 variants due to the fact that some variants could be identified as basis for several HLA-binding epitopes. Due to very rare representation of HLA-A*02:11 in German population, 4/23 peptides could not be tested. PBMC = peripheral blood mononuclear cell, ctrl. = control, NGS = next generation sequencing, seq = sequencing, AF = allele frequency, HLA = human leucocyte antigen. Source: Blaeschke, Paul *et al.* (2019)

both treated for MB at the Children's University Clinic of Tübingen. Their characteristics are depicted in Table 3. Patient 1 was diagnosed with infratentorial MB and infiltration of the vermis in August 2012 at the age of 11 months. Tumor sample was obtained from a biopsy prior to neo-adjuvant chemotherapy and tumor resection. Despite ongoing chemotherapeutic treatment, the patient relapsed in April 2014 with meningeal tumor spreading and underwent resection of relapsed tumor in September 2014. She was found in remission at date of last follow-up in September 2016. Patient 2 was diagnosed with anaplastic infratentorial MB, infiltrating the cisterna ambiens, and primary temporal metastases on the right side in

January 2014 at the age of 13 years and 8 months. Tumor sample was obtained from tumor resection which was performed in January 2014. Chemo- as well as radiotherapy were initiated later the same year. However, he experienced relapse in July 2015, underwent surgery but died two months later. Both patients' therapy-naïve tumor tissue and control material (peripheral blood) were cryopreserved.

1.2 Detection of tumor-specific variants by next generation and deep sequencing

To identify tumor-specific mutations in resected tumor tissue, next generation sequencing (NGS) of the exome was performed. Patient's PBMCs were used as control tissue. 27 tumor-specific DNA variants were detected in patient 1 and 45 in patient 2 (116). Next, all variants were excluded which had an allele frequency (AF) lower than 5 % (detection limit) and/or less than 20 reads which resulted in 25 remaining variants from patient 1 and 42 from patient 2. AF refers to the percentage of reads in which a particular variant can be found. Depth means the amount of reads performed on a variant. In the next step, variants from non-coding sites or which were based on alternative splicing were excluded. After that, 11 variants were maintained in patient 1 and 25 in patient 2. Eventually, all variants with synonymous mutations were excluded since they would not provoke an exchange of amino acid. This led to a remaining number of 9 variants in patient 1 and 22 in patient 2 (Table 5). At this point, variants' AFs in patient 1 ranged from 5.4 to 34.5 %, most of them located slightly above detection limit only, whereas in patient 2 they ranged from 25.3 to 62.3 %. Depth performed in tumor DNA amounted to approx. 30 – 300 reads in both patients.

In order to examine transcription levels of found mutations, RNA NGS of tumor tissue was performed. Criteria of AF and depth for detection of an RNA variant were identical as described above for DNA variants. Unfortunately, RNA quality was poor and only three tumor-specific DNA variants were confirmed on RNA level: PDCD10 in patient 1 (AF: 14.9 %, depth: 47 reads) and INSM1 (AF: 24 %, depth: 25 reads) as well as PTEN (AF: 94 %, depth: 18 reads) in patient 2.

Table 4: Detected DNA and RNA variants from NGS and deep sequencing.

Only variants which led to HLA-binding peptides are listed. Thresholds defining detected variants (marked with **x**) were allele frequencies of $\geq 5\%$ and coverage of ≥ 20 reads (non-detected variants are marked with **-**). However, MAX gene had a low allele frequency in deep sequencing (*****). Some variants could not be amplified and therefore not be sequenced (**n/a**). RNA sequencing was performed to assess expression level of variants. NGS = next generation sequencing, Seq = sequencing. Adapted from Blaeschke, Paul *et al.* (2019)

Mutated gene	NGS		Deep Seq	
	DNA	RNA	DNA	RNA
Patient 1				
MAX	x	-	x*	x*
PAPD5	x	-	x	x
PDCD10	x	x	x	x
Patient 2				
ATXN1	x	-	x	x
HAL	x	-	x	-
INSM1	x	x	n/a	n/a
LOXHD1	x	-	x	-
MUC4	x	-	x	-
NEU2	x	-	x	x
PCSK9	x	-	x	n/a
RNF165	x	-	x	x
SCYL3	x	-	x	x
SVIL	x	-	x	x
TSEN54	x	-	x	x
VIT	x	-	x	-

Table 5: DNA and RNA sequencing data of both next generation and deep sequencing runs.

Selection of variants in each patient is depicted after exclusion of nonsynonymous mutations and before binding-affinity prediction. Detection thresholds are AF \geq 5 % (0.05) and depth \geq 20 reads. Abbr. = abbreviated, AF = allele frequency, n/a = not applicable, NGS = next generation sequencing. Source: Blaeschke, Paul *et al.* (2019)

Mutated gene (abbr.)	Next Generation Sequencing				Deep Sequencing			
	Tumor DNA		Tumor RNA		Tumor DNA		Tumor RNA	
	AF	depth	AF	depth	AF	depth	AF	depth
Patient 1								
C5orf60	0.0714	227	n/a	n/a				
F5	0.0543	132	0	3				
KMT2D	0.3333	31	0.3333	12				
MAX	0.0667	91	0.0159	126	0.0225	56824	0.0283	6012
PAPD5	0.0559	143	n/a	n/a	0.0587	60665	0.0504	22427
PCDHB10, PCDHB9	0.3448	29	0.4	5				
PDCD10	0.1579	57	0.1489	47	0.1179	83913	0.0966	14094
ZAN	0.0662	307	n/a	n/a				
ZNF599	0.0642	111	0	1				
Patient 2								
ABHD4	0.3415	83	n/a	n/a				
ATXN1	0.3911	179	1	1	0.3767	172947	0.1994	15283
CC2D2A	0.4375	48	1	1				
C4orf51	0.3661	127	n/a	n/a				
HAL	0.3265	49	n/a	n/a	0.4241	69902	0.0012	13644
INSM1	0.5253	99	0.24	25	n/a	n/a	n/a	n/a
LILRB1	0.3837	86	n/a	n/a				
LOXHD1	0.2529	88	n/a	n/a	0.4092	23318	0.0016	22823
MUC4	0.4667	30	n/a	n/a	0.5753	10764	0.0009	12238
NCOR2	0.4058	313	0.25	4				
NEU2	0.3721	130	n/a	n/a	0.4030	19960	0.4516	16591
PCDHB16, PCDHB9, PCDHB8	0.4128	238	0.6	5				
PCSK9	0.3967	123	n/a	n/a	0.3764	33038	n/a	n/a
PIK3CA	0.4138	58	n/a	n/a				
PLEKHA4	0.3295	88	0.3333	3				
PTEN	0.623	122	0.9444	18				
RNF165	0.3729	120	0.6	5	0.4356	28460	0.5193	17319
SCYL3, C1orf112	0.4828	87	n/a	n/a	0.3987	32648	0.2563	13318
SLC41A2	0.4103	39	0.5	2				
SVIL, LOC102724316	0.3429	105	0	1	0.4049	21980	0.4232	13499
TSEN54, LGL2	0.4364	55	0.6667	3	0.4282	26764	0.5018	15762
VIT	0.3421	77	n/a	n/a	0.4157	24602	0.0004	10700

Table 6: Characteristics of variants detected by whole exome sequencing in the two patients.

All variants leading to HLA-binding neoepitopes according to affinity prediction are included. Peptides resulting from MAX and PAPD5 (**grey frame**) could not be tested due to very low allele frequency (0.032 %) of respective HLA type in German population. Chromosome number, position on chromosome and base exchange of found mutations are depicted. The function descriptions are derived from Uniprot, Entrez Gene, CIViC summary and NCBI databases. HLA = human leucocyte antigen, NCBI = National Center for Biotechnology Information. Source: Blaeschke, Paul *et al.* (2019)

Gene	Chr.	Position of mutation	Base exch.	Function of gene	
Patient 1					
MAX	MYC Associated Factor X	14	65544747	C → T	Transcription regulator. Forms a sequence-specific DNA-binding protein complex with MYC or MAD. The MYC:MAX complex is a transcriptional activator, whereas the MAD:MAX complex is a repressor. May repress transcription via the recruitment of a chromatin remodeling complex.
PAPD5	PAP Associated Domain Containing 5	16	50250053	C → T	Has a poly(A) RNA polymerase activity and is involved in a post-transcriptional quality control mechanism. Plays a role in replication-dependent histone mRNA degradation. May play a role in sister chromatid cohesion.
PDCD10	Programmed Cell Death 10	3	167405468	C → G	Promotes cell proliferation and modulates apoptotic pathways. Important for cell migration, and for normal structure and assembly of the Golgi complex. Required for normal angiogenesis, vasculogenesis and hematopoiesis during embryonic development.
Patient 2					
ATXN1	Ataxin 1	6	16326723	C → T	Chromatin-binding factor that represses Notch signaling and binds RNA in vitro. May be involved in RNA metabolism. Associated with cerebellar ataxias.
HAL	Histidine Ammonia-Lyase	12	96380914	G → A	Cytosolic enzyme catalyzing the first reaction in histidine catabolism. Defects cause histidinemia which is characterized by increased histidine and histamine and decreased urocanic acid in body fluids.
INSM1	Insulinoma-associated 1	20	20349759	C → T	Transcriptional regulator that plays a key role in neurogenesis and neuroendocrine cell differentiation. Negatively regulates skeletal muscle-specific gene expression by inhibiting the Notch signaling pathway. Represses target gene transcription by recruiting chromatin-modifying factors. Promotes the generation and expansion of neuronal basal progenitor cells in the developing neocortex. Promotes cell cycle signaling arrest and inhibition of cellular proliferation.
LOXHD1	Lipoxygenase Homology Domains 1	18	44181236	G → A	Thought to be involved in targeting proteins to the plasma membrane. Mutations in this gene lead to auditory defects, indicating that this gene is essential for normal hair cell function.
MUC4	Mucin 4	3	195477778	C → T	May play a role in tumor progression due to repression of apoptosis and stimulation of proliferation. Seems to alter cellular behavior through both anti-adhesive effects on cell-cell and cell-extracellular matrix interactions. Plays an important role in cell proliferation and differentiation of epithelial cells.
NEU2	Neuraminidase 2	2	233899297	G → A	Belongs to a family of glycohydrolytic enzymes which remove sialic acid residues from glycoproteins and glycolipids.
PCSK9	Proprotein Convertase Subtilisin	1	55518031	G → T	Responsible for proteases that process protein and peptide precursors trafficking through regulated or constitutive branches of the secretory pathway. The encoded protein is constitutively secreted as an inactive protease into the extracellular matrix and trans-Golgi network. Plays a role in cholesterol and fatty acid metabolism.
RNF165	Ring Finger Protein 165	18	44030275	G → A	Acts as a regulator of motor axon elongation. Required for efficient motor axon extension in the dorsal forelimb. Acts by mediating ubiquitination and degradation of SMAD inhibitors.
SCYL3	SCY1 Like Pseudokinase 3	1	169824996	G → A	Encodes a protein with a kinase domain and four HEAT repeats. It might interact with ezrin, an ERM protein, and may play a role in cell adhesion and migration.
SVIL	Supervillin	10	29769712	C → T	Tightly associated with both actin filaments and plasma membranes, suggesting a role as a high-affinity link between the actin cytoskeleton and the membrane. The encoded protein appears to aid in both myosin II assembly during cell spreading and disassembly of focal adhesions.
TSEN54	tRNA Splicing Endonuclease Subunit 54	17	73519845	G → A	Encodes a subunit of the tRNA splicing endonuclease complex. The complex is also implicated in pre-mRNA 3-prime end processing. Mutations in this gene result in pontocerebellar hypoplasia type 2.
VIT	Vitron	2	37032647	C → T	Encodes an extracellular matrix protein. The protein may be associated with cell adhesion and migration. High levels of expression of the protein in specific parts of the brain suggest its likely role in neural development.

Table 7: Function of mutated genes without predicted epitopes.

For description, see Table 6. The function descriptions are derived from Uniprot, Entrez Gene, CIViC summary and NCBI databases. HLA = human leucocyte antigen, NCBI = National Center for Biotechnology Information. Source: Blaeschke, Paul *et al.* (2019)

Gene	Chr.	Position of mutation	Base exch.	Function of gene	
Patient 1					
C5orf60	Chromosome 5 Open Reading Frame 60	5	179069967	T → G	Uncharacterized. The coding status remains uncertain.
F5	Coagulation Factor V	1	169510367	T → G	Central regulator of hemostasis. It serves as a critical cofactor for the prothrombinase activity of factor Xa that results in the activation of prothrombin to thrombin.
KMT2D	Lysine Methyl- transferase 2D	12	49444377	- → G	Histone methyltransferase. Methylates Lys-4 of histone H3 (H3K4me). H3K4me represents a specific tag for epigenetic transcriptional activation. Acts as a coactivator for estrogen receptor by being recruited by ESR1, thereby activating transcription.
PCDHB10, PCDHB9	Protocadherin Beta 10 / 9	5	140573754	A → C	Potential calcium-dependent cell-adhesion protein. May be involved in the establishment and maintenance of specific neuronal connections in the brain.
ZAN	Zonadhesin	7	100350676	C → T	Binds in a species-specific manner to the zona pellucida of the egg. May be involved in gamete recognition and/or signaling.
ZNF599	Zinc Finger Protein 599	19	35250525	G → A	May be involved in transcriptional regulation.
Patient 2					
ABHD4	Abhydrolase Domain Containing 4	14	23072924	G → A	Among its related pathways are Metabolism and Glycerophospholipid biosynthesis. May have hydrolase activity and 1-alkyl-2-acetyl-glycerophosphocholine esterase activity.
CC2D2A	Coiled-Coil And C2 Domain Containing 2A	4	15559074	C → T	Component of the tectonic-like complex, a complex localized at the transition zone of primary cilia and acting as a barrier that prevents diffusion of transmembrane proteins between the cilia and plasma membranes. Required for ciliogenesis and sonic hedgehog/SHH signaling.
C4orf51	Chromosome 4 Open Reading Frame 51	4	146601519 - 146601521*	AAC → -	Uncharacterized.
IL12A, IL12A-AS1	Interleukin 12A - IL12A Antisense RNA 1	3	159711223	- → T	IL-12 is a cytokine that can act as a growth factor for activated T and NK cells, enhance the lytic activity of NK/lymphokine-activated Killer cells, and stimulate the production of IFN-gamma by resting PBMC. - IL12A-AS1 is an RNA Gene, and is affiliated with the non-coding RNA class. Diseases associated with IL12A-AS1 include Behcet Syndrome.
LILRB1	Leukocyte Immunoglobulin Like Receptor B1	19	55146187	C → T	Receptor for class I MHC antigens. Recognizes a broad spectrum of HLA-A, HLA-B, HLA-C and HLA-G alleles. Receptor for H301/UL18, a human cytomegalovirus class I MHC homolog. Ligand binding results in inhibitory signals and down-regulation of the immune response. Engagement of LILRB1 present on natural killer cells or T-cells by class I MHC molecules protects the target cells from lysis. Interaction with HLA-B or HLA-E leads to inhibition of the signal triggered by FCER1A and inhibits serotonin release. Inhibits FCGR1A-mediated phosphorylation of cellular proteins and mobilization of intracellular calcium ions.
NCOR2	Nuclear Receptor Corepressor 2	12	124915273	G → A	Transcriptional corepressor. Mediates the transcriptional repression activity of some nuclear receptors by promoting chromatin condensation, thus preventing access of the basal transcription. Involved in the regulation BCL6-dependent of the germinal center (GC) reactions, mainly through the control of the GC B-cells proliferation and survival.
PCDHB16, PCDHB9, PCDHB8	Protocadherin Beta 16 / 9 / 8	5	140563152	G → A	Potential calcium-dependent cell-adhesion protein. May be involved in the establishment and maintenance of specific neuronal connections in the brain.
PIK3CA	Phosphatidylinosi- tol-4,5-Bisphos- phate 3-Kinase Catalytic Subunit Alpha	3	178936091	G → A	PIK3CA is the most recurrently mutated gene in breast cancer, and has been found to important in a number of cancer types. An integral part of the PI3K pathway, PIK3CA has long been described as an oncogene, with two main hotspots for activating mutations, the 542/545 region of the helical domain, and the 1047 region of the kinase domain. PIK3CA, and its interaction with the AKT and mTOR pathways, is the subject of an immense amount of research and development, and PI3K inhibition has seen some limited success in recent clinical trials.

Gene	Chr.	Position of mutation	Base exch.	Function of gene	
Patient 2					
PLEKHA4		Pleckstrin Homology Domain Containing A4	19 49364921	C → T	Encodes a pleckstrin homology (PH) domain-containing protein. The PH domain is found near the N-terminus and contains a putative phosphatidylinositol 3, 4, 5-triphosphate-binding motif. Elevated expression of this gene has been observed in some melanomas.
PTEN		Phosphatase And Tensin Homolog	10 89692905	G → A	PTEN is a multi-functional tumor suppressor that is very commonly lost in human cancer. Observed in prostate cancer, glioblastoma, endometrial, lung and breast cancer to varying degrees. Up to 70% of prostate cancer patients have been observed to have loss of expression of the gene. It is a part of the PI3K/AKT/mTOR pathway and mTOR inhibitors have been relatively ineffective in treating patients with PTEN loss.
SLC41A2		Solute Carrier Family 41 Member 2	12 105260325	C → T	Acts as a plasma-membrane magnesium transporter.

Table 8: Data of *in silico* binding-affinity prediction of all synthesized mutation-specific peptides.

Binding affinity was determined by netMHCpan 2.4 database (by netMHC 3.0 when marked with **a**). Predicted affinity is depicted as IC50 value (binding affinity) with a threshold < 500 nM (< 50 nM for strong binders [**b**]). Logscores are shown (log-transformed binding affinity) with a threshold > 0.426. 4/23 peptides could not be tested due to allele frequency of 0.032 % in German population of respective HLA type (**gray**). Nine peptides induced a positive T-cell response (**+**). Since donor 10 had both HLA-B*18:01 and -B*44:02, it is unclear, which HLA type mediated response against peptides 9 and 21 (**c**). HLA = human leucocyte antigen, PBMC = peripheral blood mononuclear cell. Source: Blaeschke, Paul *et al.* (2019)

Mutated gene	Amino acid sequence	Peptide number	HLA type	Binding affinity [nM]	Logscore	No. of runs	Pos. T-cell responses
Patient 1							
MAX	SQAQILDKA	3	A*02:11	267,47	0,483	0	
	SLQGEKASQ	27	A*02:11	63	0,617	0	
PAPD5	PLWTLEEALWK	4	A*02:11	476	0,43	0	
	ALWKHKVA	28	A*02:11	10 ^{a,b}	0,781 ^{a,b}	0	
PDCD10	IASPIKEL	5	C*12:02	446.24	0.436	3	+
	IASPIKELL	6	C*12:02	499.38	0.426	3	
	LQTIKDIASPI	7	B*52:01	490	0.427	3	+
Patient 2							
ATXN1	QSAEISNNL	8	C*12:03	227.1	0.499	3	
HAL	VERASAIW	9	B*18:01	30 ^{a,b}	0.684 ^{a,b}	1	+ ^c
			B*44:02	106.13	0.569	3	
	WQADIVAAL	10	B*18:01	356.98	0.457	4	
INSM1	YADPFALV	24	A*01:01	152.7	0.535	2	
LOXHD1	LSPLSWVSV	13	C*05:01	331.96	0.463	2	
MUC4	DMRDVTAL	14	C*12:03	266.06	0.484	2	
NEU2	KTGEQRVVT	15	C*12:03	295.19	0.474	4	+
PCSK9	FTDFENVP	16	C*05:01	415.32	0.443	3	+
	DHREIEGRVMF	19	B*18:01	413 ^a	0.443 ^a	4	+
	REIEGRVMF	21	B*18:01	18.87 ^b	0.729 ^b	4	+ ^c
			B*44:02	196.35	0.512	3	
RNF165	MVVHEIQNY	23	A*25:01	420.48	0.442	3	
SCYL3	KCFFSGSM	20	C*12:03	417.17	0.442	3	
SVIL	RTDVKAYNVT	17	C*05:01	395.55	0.447	4	+
	AYNVTRMVSM	18	C*12:03	305.89	0.471	2	
TSEN54	AQMCISGF	25	C*12:03	163.55	0.529	3	+
VIT	ALNVVVVM	26	C*12:03	191.72	0.514	3	

Additional deep sequencing of DNA was performed to confirm the tumor variants found in NGS. However, only those 15 variants (3 for patient 1 and 12 for patient 2) yielding HLA-binding peptides according to *in silico* prediction (see 1.3) were included in deep sequencing testing. In patient 1, AFs of DNA variants amounted to 2.3 – 11.8 % (depth: approx. 60000 – 84000 reads). In patient 2, they ranged from 37.6 – 57.5 % (depth: approx. 11000 – 173000 reads). In sum, 3/3 variants were confirmed in patient 1 (however, MAX yielding a low AF) and 11/12 were confirmed in patient 2 (due to poor amplification of INSM1; see Table 4).

To determine the transcriptome with a second method, RNA was transcribed into cDNA, amplified and measured by deep sequencing. All 15 variants described above were included. In patient 1, AFs of RNA mutants resulted in 2.8 – 9.7 % (depth: approx. 6000 – 22000 reads). Those of patient 2 ranged from 0.1 – 51.9 % (depth: approx. 12000 – 23000 reads). On RNA level, 3/3 RNA mutants were detected in patient 1 (with a low AF in MAX-derived transcript) and 6/12 in patient 2. Regarding patient 2, 4/12 variants were below detection limit and 2/12 could not be sequenced due to unsuccessful amplification of cDNA (see Table 4).

1.3 Identification of HLA-binding candidates *via* affinity prediction databases

In order to find potentially immunogenic neoepitopes from the variants identified in NGS and deep sequencing, binders to patients' HLA types were required. For that purpose, affinity prediction databases netMHC was consulted to scan variants for appropriate epitopes. Those had to be MHC class I-binding mutant peptides with lengths of 8 to 11 amino acids. Mutant peptides whose corresponding wild-type peptides were also predicted as binders were excluded. After these steps, 8 neoepitopes remained from patient 1, derived from the 3 variants in the genes MAX, PAPD5 and PDCD10, and 25 neoepitopes from patient 2, derived from the 12 variants in the genes ATXN1, HAL, INSM1, LOXHD1, MUC4, NEU2, PCSK9, RNF165, SCYL3, SVIL, TSEN54 and VIT. In patient 1, the variants in each gene yielded more than one neoepitope and in patient 2, genes leading to several neoepitopes were HAL, PCSK9, RNF165, SCYL3, SVIL and VIT. Finally, among all 33 neoepitopes, 23 peptides were synthesized to be tested for immunogenicity, 7 deriving from patient 1 and 16 from patient 2 (Table 8).

Healthy donors were required to carry patients' HLA types predicted to present the neoepitopes. In patient 1, those HLA types were A*02:11, B*52:01 and C*12:02, in patient 2 they were A*01:01, A*25:01, B*18:01, B*44:02, C*05:01 and C*12:03. However, due to very low allele frequency of the A*02:11 type in the German population, respective peptides could not be tested. A total of 18 healthy donors were recruited for the project.

2 Induction of neoantigen-specific T-cell responses *in vitro*

The following part started with the generation of DCs and PBLs derived from healthy donors' PBMCs and coculture of PBLs with mature peptide-pulsed DCs. Then seven weekly restimulations with peptide-pulsed and irradiated autologous PBMCs were performed. At last, IFN- γ and TNF- α secretion was measured *via* flow cytometry to assess the extent of T-cell response.

2.1 Flow-cytometric analyses of CD80, CD83 and CD86 indicate DC maturity

DCs, cultivated from donor-isolated PBMCs, served as antigen-presenting cells (APCs) for induction of *de novo* T-cell responses. To ensure high extent of DCs and DC maturity, surface markers were assessed *via* flow cytometry 72 hours after maturation cocktail (Fig. 8): HLA-DR⁺/lineage⁻ cells averaged 92.5 %, representing APCs without presence of T cells, monocytes/macrophages, B cells and NK cells (116). High amount of CD83⁺/CD80⁺ cells (95.2 %) as well as CD83⁺/CD86⁺ cells (99.7 %) indicated high maturity of DCs (Fig. 7).

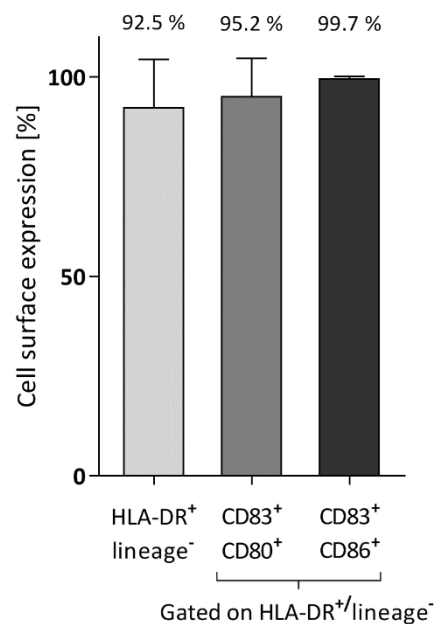


Fig. 7: High expression of CD80, CD83 and CD86 indicated maturity of DCs.

First, T cells, monocytes, B cells and NK cells were excluded by gating on HLA-DR⁺/Lineage⁻ cells. Cells from that gate showed high expression of maturity markers CD80, CD83 and CD86. Mean values \pm SD, n = 21. APC = antigen presenting cell. Source: Blaeschke, Paul *et al.* (2019)

2.2 Successful induction of *de novo* T-cell responses against 9/19 medulloblastoma-derived peptides

To assess induction of a *de novo* T-cell response, ICS was performed eight days after seventh restimulation (Fig. 9). 14 hours prior to ICS, cells were stimulated with peptide, DMSO as negative control and PMO/Ionomycin as positive control. FC was generated out of negative control and peptide-stimulated sample. A FC \geq 2 for either IFN- γ or TNF- α was defined as positive T-cell response. There were 59 tested peptide/donor combinations in total (Appendix, Table 9), with peptide 21 being tested with six donors, peptides 10, 17 and 19 with four donors, peptides 05, 06, 07, 08, 09, 15, 16, 20, 23, 25 and 26 with three donors and peptides 13, 14, 18 and 24 with two donors (116). Peptide 15 was tested twice with the same donor. Moreover, there were two peptides (09 and 21) which had been predicted to bind to both HLA B*18:01 and B*44:02.

Of the 19 mutation-specific peptides tested, there were nine which induced a T-cell response: peptides 5 and 7 (both derived from PDCD10), 9 (HAL), 15 (NEU2), 16, 19 and 21 (all three derived from PCSK9), 17 (SVIL) and 25 (TSEN54) (Fig. 10, Fig. 11, Table 8). Peptide 15 was tested a second time 21 weeks after first run with a new PBMC sample from the same donor, but a positive T-cell response could not be reproduced.

Three donors (donor 03, 07 and 10) showed more than one positive T-cell response: Donor 03 with peptides 05 and 07, donor 07 with peptides 17 and 19 and donor 10 with peptides 09 and 21.

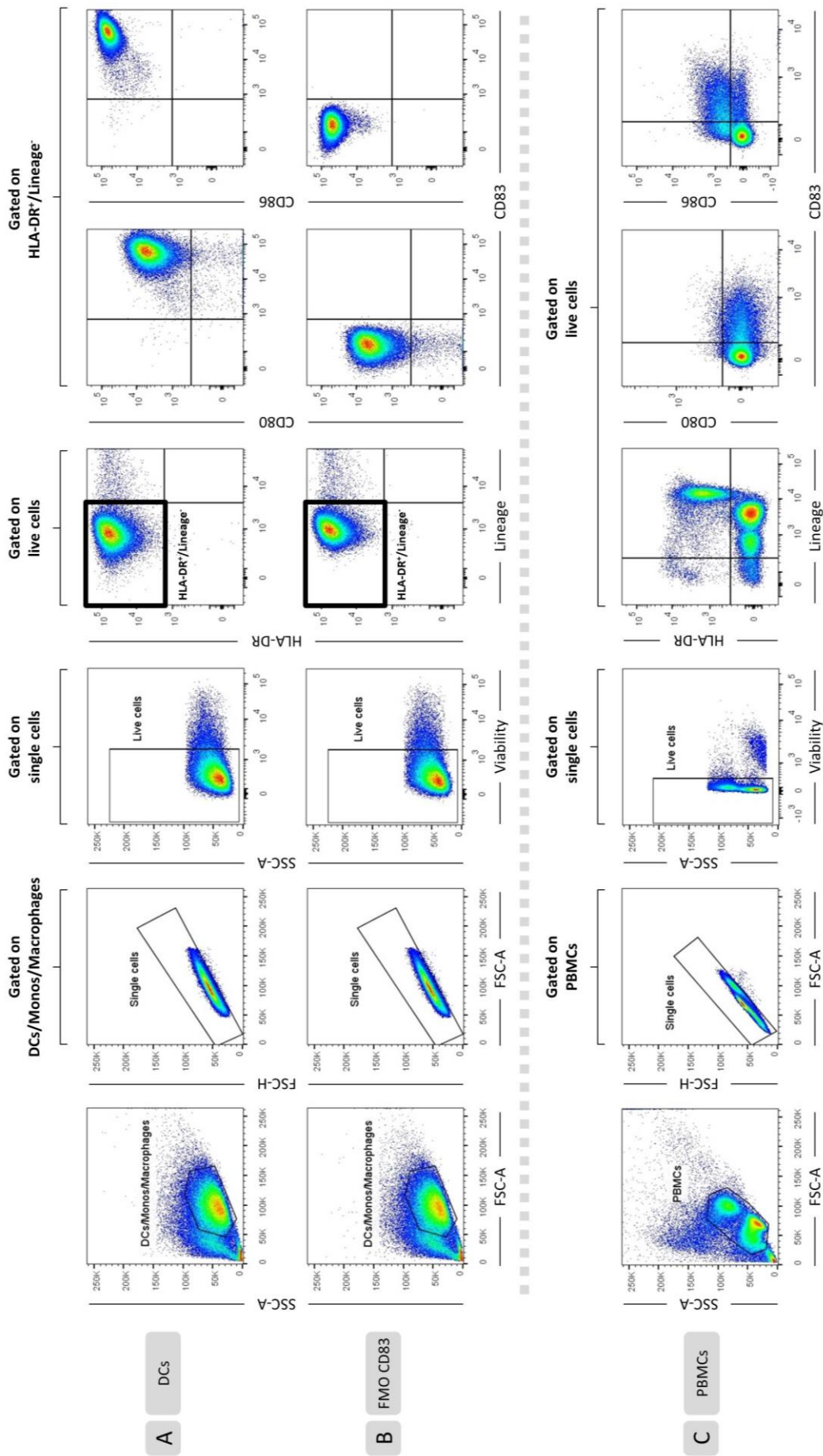


Fig. 8: Example of flow-cytometric analysis of DCs on day 11 and comparison to PBMCs. Adapted from Blaeschke, Paul *et al.* (2019)
A and B) After excluding doublets and dead cells, HLA-DR⁺/lineage⁻ cells were isolated. By that, T cells, monocytes/macrophages, B cells and natural killer cells were excluded (via lineage cocktail consisting of CD3, CD14, CD19, CD20 and CD56 antibodies) and APCs were selected (via HLA-DR antibody). Amount of DCs was measured via expression of CD80/CD86 receptors and CD83 antibody was implemented to specifically assess maturity of DCs. An FMO CD83 and an isotype control were inserted as well.
C) Same staining panel as described above was applied for unaltered PBMCs to illustrate how PBMCs are lineage⁺/HLA-DR⁻ except for monocytes/macrophages and mostly CD80⁺, CD83⁺ and CD86⁺. DC = dendritic cell, APC = antigen-presenting cell, FMO = fluorescence minus one, PBMC = peripheral blood mononuclear cell

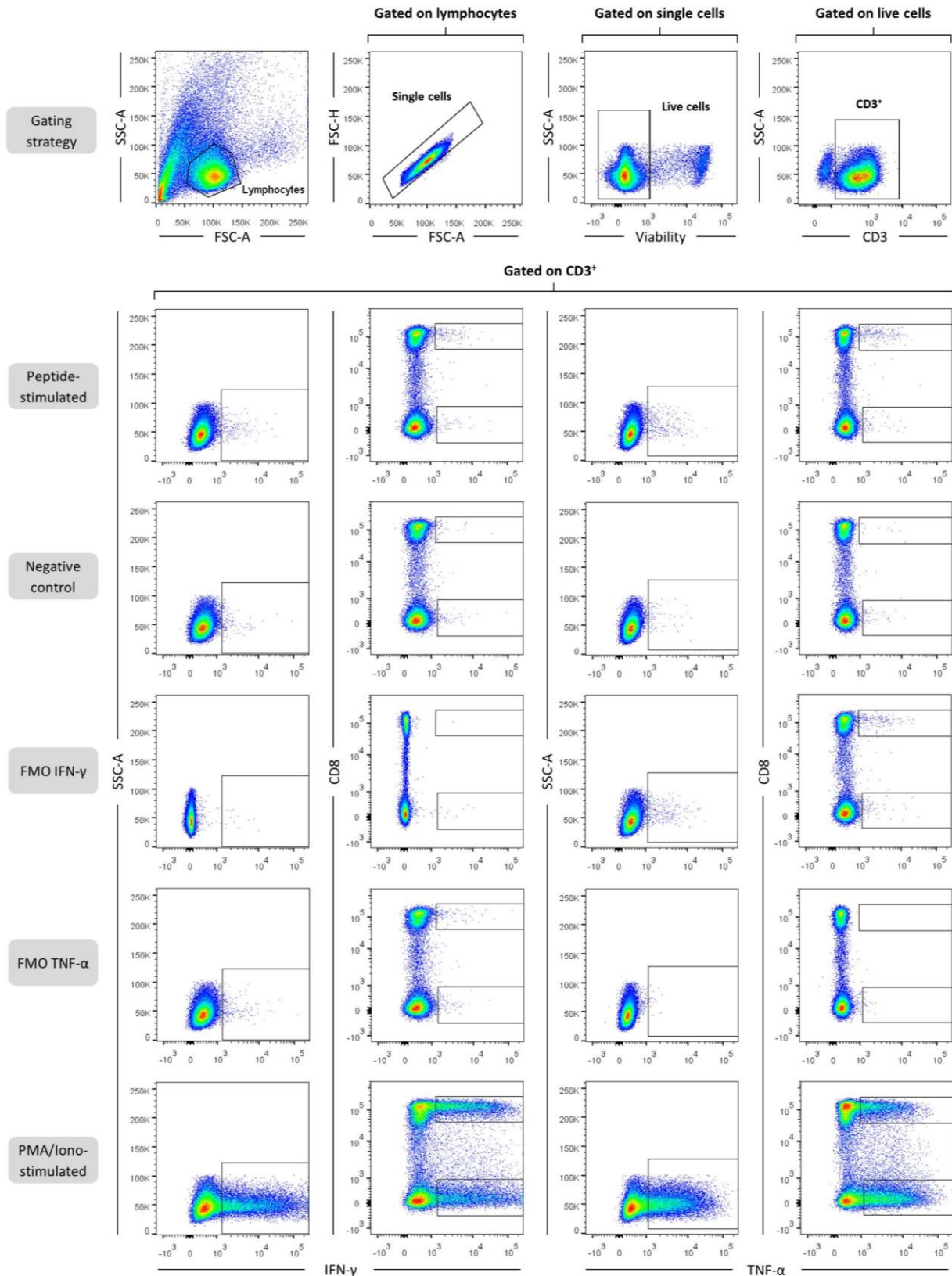


Fig. 9: Example of successfully induced T-cell response (peptide 17) measured by flow cytometry. Stimulation was performed 14 hours prior to measurement. Depicted plots are derived from peptide-treated conditions after seven restimulations. After exclusion of doublets and dead cells, CD3⁺ cells were gated. IFN-γ and TNF-α release of CD3⁺ cells as well as of CD4⁺/CD8⁺ subsets was assessed and used to generate FCs compared to negative control. FC ≥ 2 was considered a positive T-cell response. PMA/Ionomycin (positive) control and FMO controls were included. SSC = side scatter, FSC = forward scatter, FMO = fluorescence minus one, PMA = phorbol-12-myristate-13-acetate, Iono = Ionomycin, FC = fold change. Adapted from Blaesche, Paul *et al.* (2019)

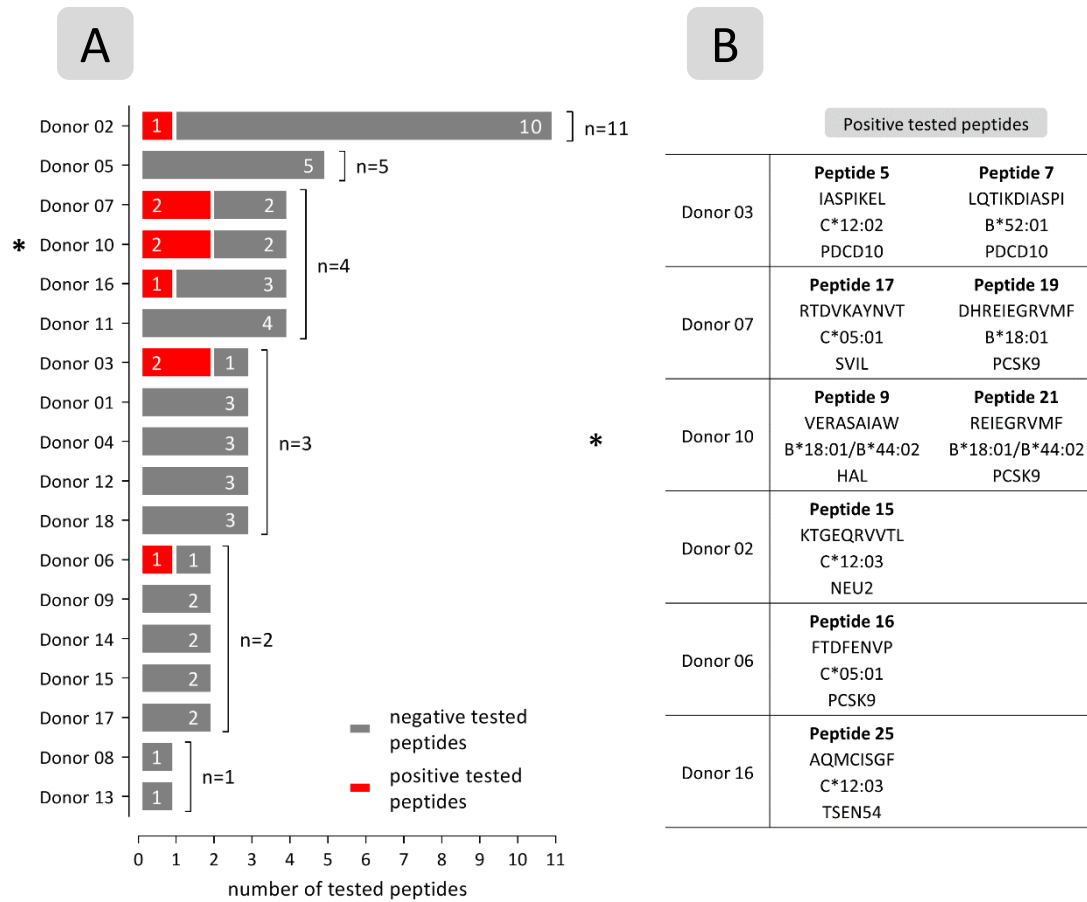


Fig. 10:

A) Number of negative and positive tested peptides per donor. Number of tested peptides was dependent on amount of isolated donor PBMCs and of number of matching HLA types.

B) Donor/peptide combinations of all positive tested peptides. Peptide numbers, their amino acid sequence, their predicted binding HLA type and the name of the underlying mutated genes from are listed. Since donor 10 had both B*18:01 and B*44:02 HLA types, it is unclear which one mediated the T-cell response against peptide 9 and 21 (*). PBMC = peripheral blood mononuclear cell, HLA = human leucocyte antigen

2.3 Mutation-specific T-cell responses were mainly caused by CD8⁺ IFN- γ secreting cells

Since cytokine release was examined separately for CD3⁺ and CD4⁺/CD8⁺ cells, T-cell responses could be assigned not only to IFN- γ and TNF- α secretion, but also to CD3⁺ cells and CD4⁺/CD8⁺ subpopulations (Fig. 11). One IFN- γ or TNF- α FC value above threshold derived of any of the three groups (CD3⁺, CD4⁺ or CD8⁺) was used to define a positive response.

In all 9/9 positive responses, CD8⁺ FC values > 2 were found whereas in 2/9 responses CD4⁺ cells produced FC values > 2 (116). IFN- γ secretion above threshold was found in 7/9 and significant secretion of TNF- α in 5/9 responses. However, CD3⁺ gated cells were able to detect only 3/9 responses. Among those, IFN- γ accounted for 1/3 and TNF- α for 2/3.

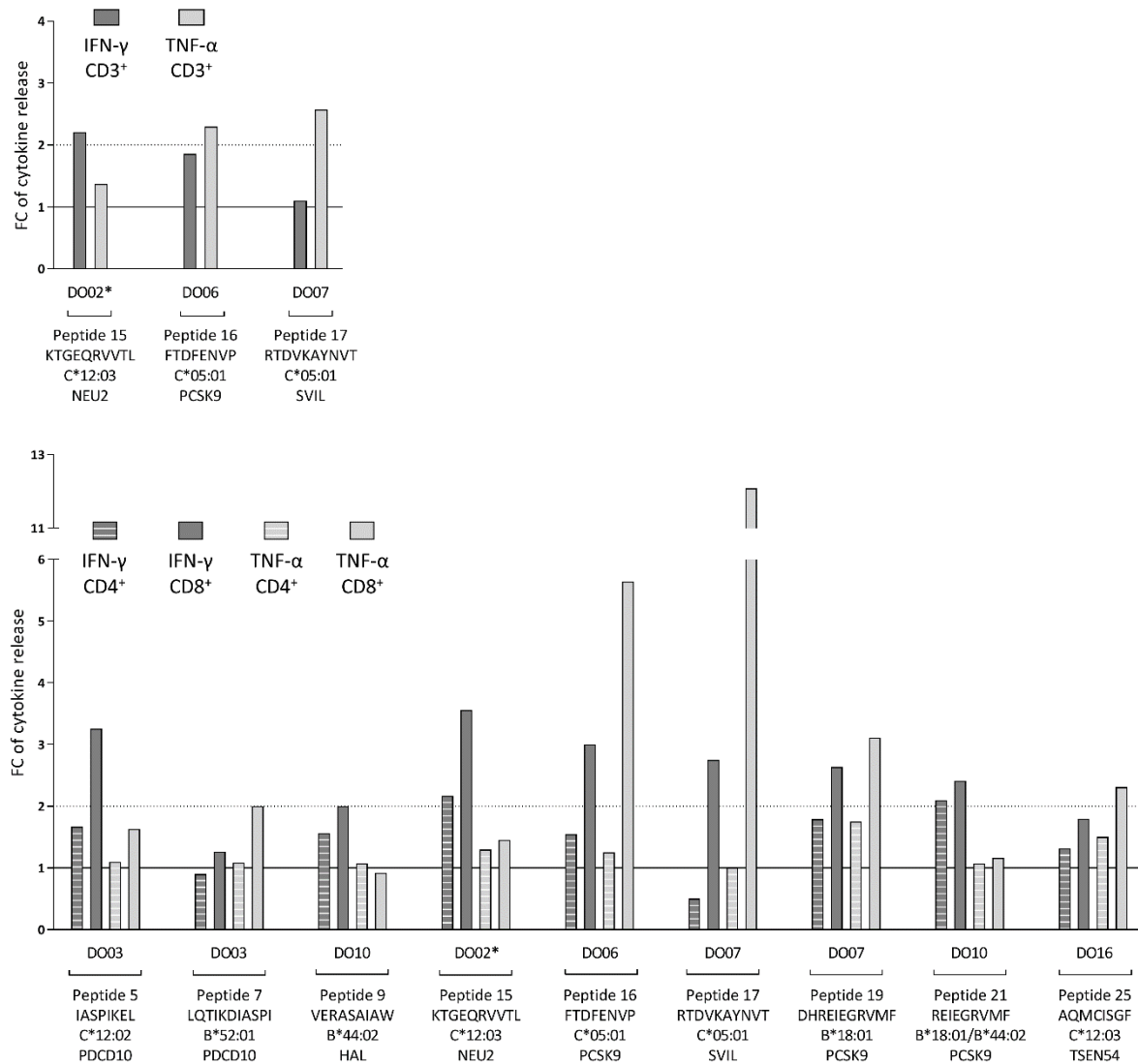


Fig. 11: Positive T-cell responses defined by CD3+ cells only or CD4+/CD8+ subpopulations.

Cytokine release induced by positive tested peptides is depicted as FC compared to negative control. When only considering FCs of CD3+ cells, there were a total of three detected positive T-cell responses whereas there were nine when taking into account FCs of CD4+/CD8+ subpopulations. Donors, peptide numbers, their amino acid sequence, their predicted binding HLA type and the name of the mutated genes from which they were derived are listed. Results from peptide 15 are derived from donor's first PBMC donation (*). FC = fold change, DO = donor. Adapted from Blaesche, Paul *et al.* (2019)

Regarding the amount of FC values above threshold among cells gated to CD4+ and CD8+, there were a total of 14 values, composed of 12/14 CD8+-mediated and 2/14 CD4+-mediated ones. CD8+ cells averaged an FC of 3.73 (2.00 – 12.08) and CD4+ cells an FC of 2.13 (2.10 – 2.17). As to the cytokine proportions, 9/14 values derived from IFN-γ and 5/13 from TNF-α secretion. Mean IFN-γ FC amounted to 2.65 (2.00 – 3.56) and that of TNF-α to 5.03 (2.00 – 12.08). There were an additional 3 values above threshold, derived from CD3+ gated cells.

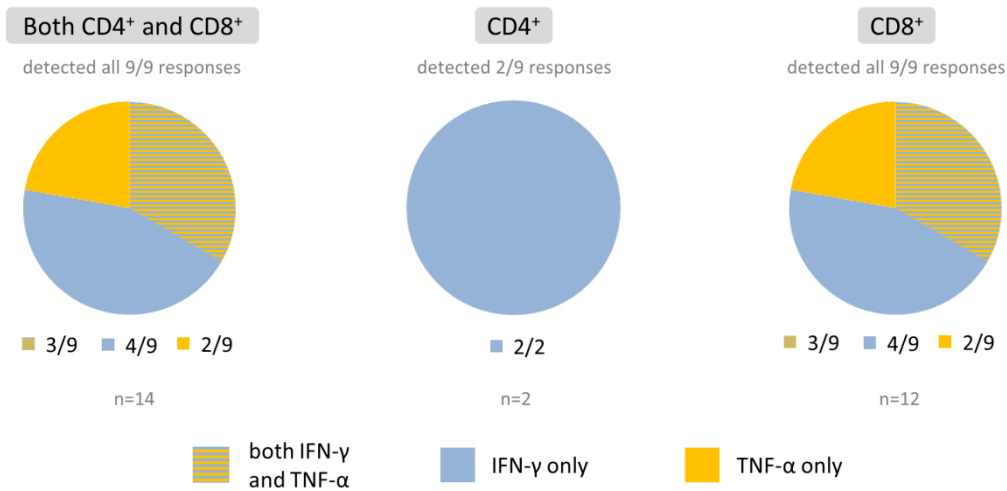


Fig. 13: Proportion of IFN- γ and TNF- α release of CD4⁺ and/or CD8⁺ subpopulation in positive T-cell responses.

Nine *de novo* T-cell responses were found, generated by a total of 14 FC values derived from IFN- γ /TNF- α release by CD4⁺/CD8⁺ cells. By definition, one cytokine secretion FC value of ≥ 2 compared to negative control was sufficient for a positive response. IFN- γ -secreting CD8⁺ cells induced the majority of T-cell responses. Resp. = response, FC = fold change

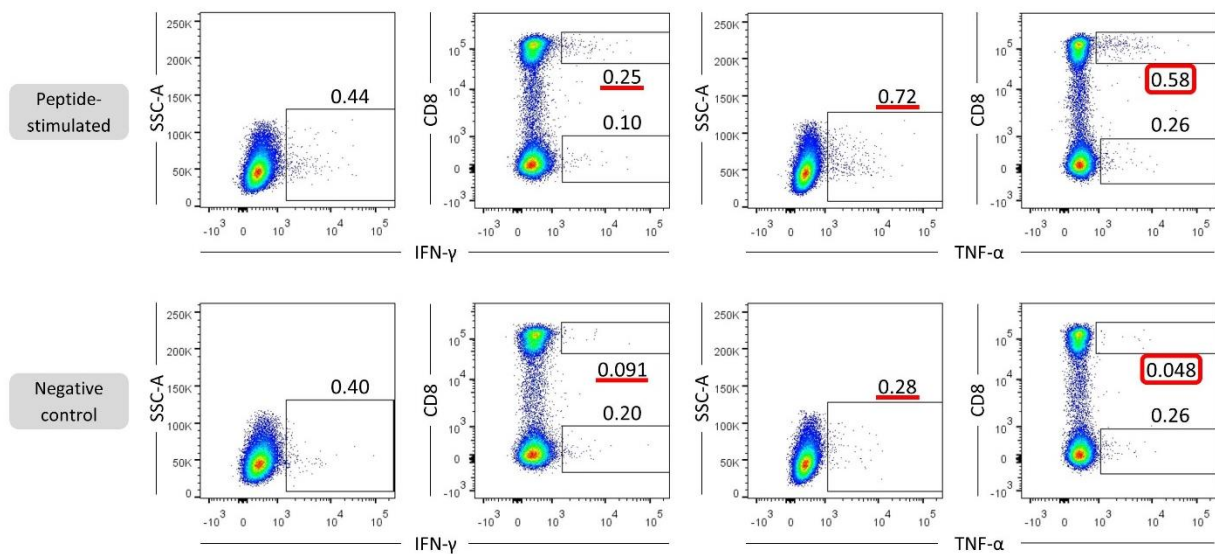


Fig. 12: Strong T-cell response against peptide 17 in flow-cytometric analysis.

Peptide 17 (SVIL) showed the highest TNF- α release FC in CD8⁺ cells compared to the negative control among all T-cell responses with an FC value of 12.08 (0.58/0.048; red frames). Further FCs above threshold were found in CD8⁺ IFN- γ releasing as well as CD3⁺ TNF- α releasing cells (underlined in red). FC = fold change. Source: Blaeschke, Paul *et al.* (2019)

2.3.1 SVIL-derived peptide 17 induced strongest T-cell response

When tested with donor 07, peptide 17 (derived from gene SVIL) induced a strong T-cell response regarding TNF- α secretion of CD8⁺ cells with an FC of 12.08, generated from frequencies 0.58 (peptide-stimulated) and 0.048 (negative control) (116). The IFN- γ secretion FC of CD8⁺ cells was 2.75. The CD4⁺ cell TNF- α FC and CD4⁺ cell IFN- γ FC however did not reach the threshold of 2 (Fig. 12).

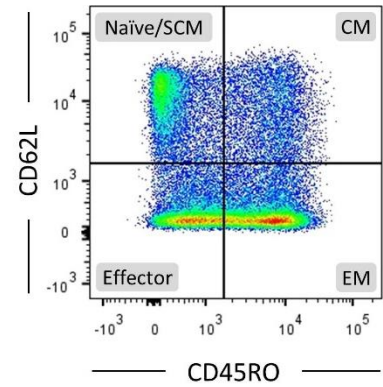


Fig. 14: Determining T-cell phenotypes. SCM = stem cell memory, CM = central memory, EM = effector memory. Source: Blaeschke, Paul *et al.* (2019)

2.4 Impact of T-cell phenotype on induction of mutation-specific T-cell responses

Phenotypes of T cells were examined by implementing antibodies labeling CD62L and CD45RO surface markers in ICS. Phenotypes were determined as follows (Fig. 14): Naïve/stem cell memory (SCM) cells correspond to CD62L⁺/CD45RO⁻ cells, central memory (CM) cells to CD62L⁺/CD45RO⁺, effector memory (EM) cells to CD62L⁻/CD45RO⁺ and effector cells to CD62L⁻/CD45RO⁻ cells.

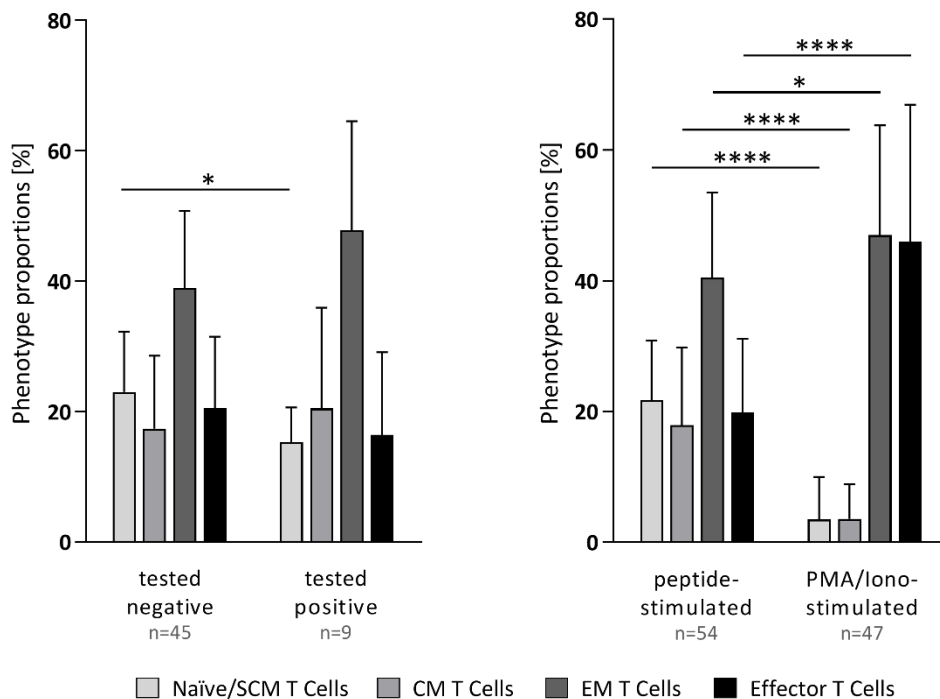


Fig. 15: T-cell differentiation on final ICS.

T-cell phenotypes on final ICS measurements determined *via* CD62L and CD45RO. On the left, peptide-stimulated T cells are compared. Significant differences were found in naïve/SCM cell amounts. On the right, peptide-stimulated T cells are compared to T cells stimulated which PMA/ionomycin. The latter showed a significant down-regulation of CD62L, resulting in decreased amount of naïve/SCM and CM cells. Mean values \pm SD. * $p < 0.05$, **** $p < 0.0001$. PMA = phorbol-12-myristate-13-acetate, Iono = ionomycin, SCM = stem cell memory, CM = central memory, EM = effector memory. Adapted from Blaeschke, Paul *et al.* (2019)

When pooling all values derived from negative and positive tested peptides, naïve/SCM cell proportions showed significant differences (Fig. 15, left): They amounted for 23.03 % of all phenotypes in conditions with negative tested peptide as compared with 15.32 % in those with positive tested peptide (116). To assess stimulation capacity of T cells, different conditions were stimulated with positive control PMA/Ionomycin 14 hours prior to ICS. In all measurements, a down-regulation of CD62L could be observed (Fig. 15, right).

D Discussion

Medulloblastoma is the most common malignant pediatric brain tumor (117). Treatment is challenging and is accompanied by long-term side effects affecting the developing child. Therefore, new therapeutic approaches are needed. The aim of the present study was to investigate the immunogenicity of tumor-specific peptides derived from two pediatric MB patients. DCs and lymphocytes were gained from healthy donors' PBMCs, the lymphocytes cocultivated with peptide-pulsed DCs and finally induction of a *de novo* T-cell response was measured *via* IFN- γ and TNF- α release. Nine of nineteen peptides were able to induce T-cell responses. The results indicate that MB tissue harbors immunogenic epitopes that can potentially serve as targets for immunotherapy. This paves the way for further studies that can lead to therapeutic application in the clinic: One potential future approach being peptide vaccination where tumor-specific peptides are synthesized and administered to boost the endogenous immune response. ATT is another highly individualized future treatment option: At first, it would require the identification of a tumor-reactive TCR in a positive T-cell response. This TCR could then be sequenced, cloned and transduced into T cells which would be re-administered to the patient.

1 “Reverse immunology” for identification of tumor-specific neoepitopes

The neoepitopes in this project were acquired by “reverse immunology” (118): By whole exome sequencing of freshly isolated tumor and healthy (control) tissue from two MB patients, somatic mutations in the tumors were identified. Patients' PBMCs served as tumor-matching controls which is appropriate for non-hematologic cancer entities (119). Within the detected variants, HLA-binding peptides containing the mutations were determined *in silico*. This concept allows identifying a large antigen reservoir since it takes all neoepitopes into account that could potentially be derived from genes with tumor-specific mutations. However, it is not equally reliable compared to direct epitope acquirement methods as it cannot consider all steps between the transcription of a mutation and the expression of its analogous antigen. For instance, discrepancy between *in silico* and *in vivo* neoepitopes can occur as proteasomal cleavage can destroy antigens (120) and predicting MHC binding of peptides containing cysteine has shown to be problematic (121). In order to verify the variants identified by whole exome sequencing, deep sequencing of amplified DNA was performed. It achieved a mean depth of > 45000 reads and confirmed 93 % of the variants.

Determining suitable cancer neoepitopes is often performed with a focus on MHC class I-binding antigens and therefore on the CD8⁺ T-cell axis (122, 123), further discussed in 3. Accordingly, selection of neoepitopes for this project was made exclusively using MHC class I-binding affinity prediction. The databases consulted for this purpose use algorithms based on experimental knowledge of proteasomal cleavage, peptide transport to the endoplasmic reticulum and MHC binding (124). A cut-off of 500 nM in terms of netMHC affinity score was applied. Although Paul *et al.* recently showed that each HLA allele has unique binding affinities to its epitopes and therefore different thresholds, the value of 500 nM is

commonly used and a suitable universal threshold (125). Peptides with an affinity of ≤ 50 nM were considered strong binders. Only PAPD5 and PCSK9 peptides were predicted strong binders. However, PAPD5 could not be tested due to very low allele frequency (0.032 %) of respective HLA type in German population. A T-cell response could be induced against the PCSK9 peptide. Otherwise we could not observe a correlation between predicted affinity and T-cell response. However, regarding ATT, Engels *et al.* showed the significance of high affinity of peptides for MHC molecules (126): Only high-affinity peptide-MHC interactions resulted in effective tumor eradication by T cells.

Peptide length was set to be between 8 and 11 amino acids. This corresponds to the range of epitope lengths commonly binding to MHC class I molecules, which is 8 – 10 amino acids (10). The MHC class I molecule's antigen-binding groove is closed at each end and restricts binding to short and specific peptides with conserved anchor residues. Most of those MHC molecules have a strong preference for binding nonamer peptides (127). This implies, however, that there is a considerable bias towards peptides of said length, since more than 73 % of the database-underlying data apply to nonamers (127). That leads to impaired accuracy of peptide binding affinities containing more or less than nine amino acids. On the other hand, MHC class II molecules are open at both ends, allowing peptides to bind with an approximate length of 11 to 30 amino acids (11). Kreiter *et al.*, who found high amounts of immunogenic neoepitopes in murine tumor models using 27mer peptides, suggest this was due to the less strict conditions required for peptide-binding to MHC class II molecules (128).

Not only is the peptides' length critical for MHC binding: HLA-B type has demonstrated to bind a more diverse repertoire of self-peptides, derived from a larger amount of source proteins (129). Schellens *et al.* argue that the HLA-B molecules might therefore have an increased chance of presenting immunodominant peptides and be associated with immune responses more often (129). Furthermore, HLA-B might have a superior impact on the outcome of various infectious diseases, inflammatory conditions but also malignancies compared to HLA-A (129).

A mutant HLA-binding neoepitope was only selected whenever its wild-type counterpart was not predicted to bind to the HLA type. Binding properties especially depend on amino acids located in the anchor positions within the MHC-binding groove (130). It has been shown that peptides derived from mutations—therefore referred to as facilitating mutations—may be more effective in eliciting specific T-cell responses than their wild-type equivalent due to higher binding affinity of the mutant peptide (122, 131). This is due to competition between mutant and wild-type peptide in terms of binding to the MHC molecule in the endoplasmic reticulum and endosomes.

In order to determine to which extent DNA variants were detectable on transcriptome level, RNA from the tumor samples was analyzed by whole exome sequencing. To verify the findings, RNA was transcribed into cDNA, amplified and measured by deep sequencing. In whole exome sequencing, a total of 3 variants were verified on RNA level whereas in deep sequencing 9/15 variants could be confirmed. This relatively small amount of expressed mutations is in line with the findings of Jones *et al.* They found 48 % of non-

synonymous mutations represented on RNA level concluding that only very few driving hits are required to generate MB (104). Since mRNAs have a short lifetime they might not genuinely represent expression *in vivo*. In addition, Cohen *et al.* were able to induce neoepitopes-specific T-cell responses based on whole exome sequencing data only (119). For both reasons, variants not detectable on RNA level were nevertheless included into the testing.

2 DCs are crucial for *de novo* T-cell responses and for immune regulation

DCs are the essential APCs regarding the induction of *de novo* T-cell responses. As classical professional APCs, constitutively expressing MHC class II molecules, they localize to secondary lymphoid organs in order to prime naïve CD4⁺ T cells (132). However, *via* cross-presentation they interact with and promote CD8⁺ cells by presenting them (tumor) antigen on their MHC class I receptors (133). Thus, DCs induce rapid activation of tissue-resident memory CD8⁺ T cells upon re-infection (134). In this project, DCs were generated *in vitro* from monocytes originating from healthy donors' PBCMs, achieving a maturity of > 92 %. Those monocyte-derived DCs (mo-DCs) also constitute the major proportion among DCs during inflammation and therefore in the inflammatory environment of tumors (135). Tang-Huau *et al.* recently showed that both mo-DCs obtained from human ascites and generated *in vitro* from monocytes are efficient at cross-presentation (135). In a murine experiment, Kuhn *et al.* reported that mo-DCs isolated by depleting other CD11c⁺ cells are sufficient for induction of tumor-specific CD8⁺ T cell responses and successful tumor immunity (136).

In addition, DCs are critical for immune homeostasis and thus for prevention of overactivity and autoimmunity. They induce the differentiation of CD4⁺FOXP3⁺ regulatory T cells (Tregs), a T-cell subset essential for peripheral tolerance and important for tumor escape. The tolerogenic effect of DCs is also promoted by the tumor microenvironment: Vascular endothelial growth factor (VEGF) is released by tumors and has suppressive effect on dendritic cell differentiation (137). In addition, IL-6 and macrophage colony-stimulating factor (M-CSF), which are produced by tumors, suppress monocyte-induced differentiation toward DCs (138).

3 CD4⁺ and CD8⁺ T cells play ambiguous roles in eliciting T-cell responses

In the final ICS measurement, cytokine release was assessed to define positive T-cell responses. Since epitope-binding affinity was predicted for MHC class I molecules, responses of CD8⁺ T cells were the main focus. As expected, CD8⁺ was the dominant T-cell subset, secreting cytokines above threshold in all 9/9 final elicited responses. CD4⁺ cells, however, were positive in 2/9 responses. The majority of responses was mediated by IFN- γ .

Concerning the proportional contribution of CD4⁺ and CD8⁺ T cells in mounting an effective immune response, notions differ considerably. One established hypothesis says that CD4⁺ T cell help is needed for the differentiation of cytotoxic CD8⁺ T cells (139-141) and a successful and long-lasting CD8 immune

response (142). Naïve CD4⁺ cells are differentiated along the Type 1 helper T cell (Th1) subset which is the most favorable one for tumor control (143). This process is mediated by IL-12 which is released by DCs upon antigen presentation. Th1 cells enhance the development of CD8⁺ cells through epitope spreading. They promote DCs *via* the CD40 receptor and thus activate CTLs *via* cross-priming and cross-presentation (144). IFN- γ is secreted which further amplifies Th1-cell development and has a direct toxic effect on tumor cells (145).

However, CD8 responses can be robust without CD4 help. While CD8⁺ cells in the absence of CD4⁺ T cells can be impaired during viral or bacterial infections (146, 147), the absence of CD4⁺ cells may even improve CTL-mediated cancer control: After complete ablation of CD4⁺ helper cells in a murine melanoma mouse model, Côté *et al.* could not observe impaired development of an antitumor memory CD8 response (148). They even reported increased count of CD8⁺ cells as well as IFN- γ production possibly due to Treg ablation.

On the other hand, recent findings indicate a dominance of CD4⁺ T cells: Kreiter *et al.* suggest that antitumor activity might rather be conferred by CD4⁺ than CD8⁺ T cells (128). In three independent murine tumor models they showed immunogenicity of numerous tumor-specific antigens. The tumor entities comprised melanoma, colon carcinoma and breast cancer. Analyzing the involved T-cell subsets, they found CD4⁺ cells to be responsible for most of the T-cell responses in all three tumor models. The essential role of CD4⁺ cells and MHC class II-associated epitopes was also demonstrated by Tran *et al.* They found neoepitope-specific CD4⁺ Th1 cells among TILs in metastatic cholangiocarcinoma patients. Upon expansion and re-administration of those cells to the patients they could achieve tumor regression (30).

In this project, only CD8⁺ T cells were taken into account for eliciting T-cell responses by exclusively considering the healthy donors' MHC class I molecules. This is because of the major difference between existing *in silico* prediction tools for epitope-binding of MHC class I and II: Methods to predict MHC class I-restricted peptide binding have higher performance compared to MHC class II (149). This is due to several reasons: MHC class II molecules are highly polymorphic (150) and MHC class II-binding peptides have variable lengths due to the MHC molecule's open binding groove at both ends (151).

4 Several immunogenic peptides are derived from genes with potential impact on tumorigenesis

Tumor samples were taken from two patients suffering from MB. In both cases it was high risk MB including either young age (patient 1) or primary metastasis (patient 2). MB is a cancer entity of minimal mutational load (29). Analysis of 92 MB cases in a study yielded a mutation rate of 0.35 non-silent mutations per megabase (106). This contrasts with high immunogenic tumors in adults such as malignant melanoma, which shows a mean of > 10 mutations per megabase (29). Generally, mutational burden in tumors is known to increase significantly with age (152). In line with this, Jones *et al.* found a positive

correlation between patient age and mutation rate (104). Both findings are consistent with the higher amount of variants found in patient 2 in the present project.

In this project we analyzed the detected mutations in terms of their potential influence in tumor formation and growth. Since samples were taken before chemo- or radiation therapy, the mutations found in the tumor were not induced by therapeutic intervention. MB shows strong genetic heterogeneity with most mutated genes only appearing in single cases (104), as was observed in this project. In contrast, in pediatric glioblastoma frequently recurring hotspot mutations have been identified (104). However, there are some known mutated genes described in MB such as *CTNNB1*, *PTCH1*, *MLL2*, *SMARCA4* and *TP53* (104, 106).

For patient 1, a tumor-specific mutation in Programmed Cell Death 10 (PDCD10) was detected. Highlighting its function is particularly interesting as two peptides derived from this variant induced a specific T-cell response. PDCD10 encodes a highly conserved protein associated with cell proliferation and apoptosis (153). Its crucial role in apoptosis was shown by Chen *et al.*: When overexpressed in a cell line by transfection, respective cells showed increased apoptosis *via* caspase-3 activation (153). Consequently, overexpressed PDCD10 containing a point mutation resulted in reduced cell loss compared to the PDCD10 wild type (153). Moreover, Lauenborg *et al.* described the constitutive expression of PDCD10 in malignant T cells, found in cutaneous T cell lymphoma (154). However, they reported a relatively high expression in non-malignant T cells as well, in this case protecting them against apoptosis and promoting cell proliferation. Another critical function of PDCD10 concerns vascular development: He *et al.* reported that PDCD10 stabilizes the vascular endothelial growth factor receptor 2 (VEGFR2) in response to stimulation by VEGF (155). Mice lacking a normal PDCD10 gene died at embryonic stage due to defects in angiogenesis. In addition, mutants of PDCD10 in human patients were equally unable to stabilize VEGFR2 which facilitated its endocytosis and resulted in signaling defects. In consistence with this role, mutations in PDCD10 are associated with cerebral cavernous malformations (156).

In patient 2, all three peptides derived from Proprotein Convertase Subtilisin/Kexin Type 9 (PCSK9) induced a positive T-cell response. Its encoded protein plays a role in the regulation of low-density lipoprotein (LDL) receptors (157). Mutations in PCSK9 are consequently associated with disorder in cholesterol and fatty acid metabolism. This gene has not yet been described in tumorigenesis of MB although it has been associated with an anti-apoptotic effect in a study by Xu *et al.* When transfecting PCSK9 small interfering (si)RNA into a lung cancer cell line, they observed increased induction of apoptosis and therefore anti-tumor activity (158).

Mutations were moreover found in the genes Phosphatidylinositol-4,5-Bisphosphate-3-Kinase Catalytic Subunit Alpha (PIK3CA) and Phosphatase And Tensin Homolog (PTEN) in patient 2. Neither resulted in neoepitopes predicted to bind MHC class I, but both are well-known in tumorigenesis: The PI3K/Akt signaling pathway with its PIK3CA-derived protein phosphoinositide 3-kinase (PI3K) is involved in the development of several tumor entities. It is the most recurrently enhanced pathway in breast cancer

(159). Additionally, PI3K mutations were found in other malignancies such as lung and colorectal cancer (160, 161) but also in a variety of brain tumors including pediatric MB (162). Overexpression of the p110 α protein, the catalytic subunit of PI3K, was described in MB tumors and cell lines (163). Moreover, the PI3K/Akt pathway has a well-described impact in disorders that concern brain overgrowth (164). It might also have an important role in physiological brain growth (165). PTEN, on the other hand, is a tumor suppressor gene and its gene products repress the PI3K/Akt pathway. It is frequently mutated in cancer which results in loss-of-function and consecutive increased cell growth, proliferation, and survival (166).

In addition, a mucin 4 (MUC4) mutation was detected in patient 2. MUC4 is associated with cell proliferation and inhibition of apoptosis (167). It plays a role in several cancer entities such as ovarian, pancreatic and breast cancer (168-170). However, its impact in MB has not yet been described.

5 Future therapeutic approaches include peptide vaccination and adoptive T-cell transfer

Immunotherapeutic approaches including immune checkpoint inhibition, adoptive T-cell transfer and peptide vaccines have revolutionized cancer treatment. However, in MB, immunotherapeutic approaches could not yet achieve as convincing results as in non-pediatric high immunogenic tumors such as malignant melanoma where immunotherapy was introduced decades ago (77). A promising study involving ATT in lymphodepleted medulloblastoma mice showed tumor regression without any neurological dysfunction upon infusion of TILs which were activated *ex vivo* before administration (171). Naturally occurring TILs are critical for antitumor response and associated with a better outcome in several tumor entities, such as melanoma (172) and ovarian carcinoma (38). TILs have been identified in pediatric patients with MB (173). Analyzing the T-cell subsets, CD8⁺ cells constituted the main proportion (52 %) followed by CD4⁺ cells (35 %) and Tregs (2.5 %). However, no association between frequency of TILs and patients survival was observed (173).

In this project we showed feasibility of an individualized approach to detect immunogenic patient-specific neoepitopes, which can potentially be harnessed for immunotherapy. In a next step, the neoepitope-reactive TCRs could be identified in order to engineer transgenic T cells for ATT. In addition, immunogenic peptides could be synthesized and administered to the patient to boost endogenous antitumor response.

In adoptive T cell therapy, T cells are administered to patients to help eradicate malignant tumors. The infused cells can either be unaltered TILs or genetically modified T cells expressing specific TCRs or CARs (83). Whereas early ATT approaches exclusively used unmodified TILs, which additionally required time-consuming expansion and selection processes *ex vivo* (174), now highly specific transgene T cells are engineered: Peripheral blood lymphocytes are transduced with tumor-reactive TCRs that target cancer cells in tumor entities such as melanoma, which is currently being evaluated in different trials (175). The efficacy of T cells to eliminate cells has recently been shown by Leisegang *et al.* (27). They were able to eradicate a large solid tumor by TCR-engineered T cells targeting only one single cancer-specific point mutation. Despite successful tumor elimination, relapse was observed which occurred due to therapy-

induced selection of escape variants. Those variants were able to escape immune attack by down-regulation or total lack of antigen-expression. Transduction of the mutant gene into similar tumor cells could successfully reproduce tumor elimination.

According to this study, it might be inevitable to target multiple independent neoepitopes on the same tumor to reach long-lasting tumor control (27) and reduce selection of escape variants. Consequently, in tumors such as MB, heterogeneity can contribute to low allele frequencies and thus lead to decreased antitumor response. Therefore, targeting a variety of neoepitopes might be essential for successful tumor elimination. Moreover, mutational burden has an influence on immunotherapeutic effects: In a recent study, immune checkpoint blockade yielded higher response rates in tumors with high mutational burden, especially examined among melanoma and non-small cell lung cancer (NSCLC) (176). However, when combining blockade of several checkpoints, this correlation was not observed. In fact, another study analyzing immune checkpoint blockade of NSCLC adenocarcinoma detected that a combination of high mutational burden and low neoantigen intratumor heterogeneity led to longer survival rates than either variable alone (177).

Peptide vaccination aims at inducing an endogenous immune response *via* administration of tumor antigens (178). It has successfully been applied in different settings: In patients with pancreatic or colorectal cancer, a mutant ras peptide was administered leading to specific T-cell responses and increased overall survival in the responders (179). In glioblastoma patients with total tumor resection and chemoradiation, a vaccine was used which consisted of the mutated epidermal growth factor receptor variant III. It was administered in addition to adjuvant temozolomide and resulted in improvement of progression-free and overall survival (180).

Epitope loss can be challenging not only for adoptive T-cell transfer but also for peptide vaccination, partly due to deficiency in the antigen processing machinery (181). To solve this problem, the generation of multi-epitope vaccines has been proposed to increase breadth and diversity of neoantigen-specific T cells and to include MHC class II-restricted peptides to involve CD4⁺ responses (67, 182, 183). Vaccination with long peptides has proven to induce a stronger immune response, implying a delayed but sustained CTL response (184). This may be due to the necessary processing of long peptides by APCs compared to short peptides that elicit a CD8⁺ T cell response only (185). Another issue of peptide vaccines, observed in several cases, is their potential to induce peripheral T-cell tolerance and even tumor progression (68, 186). T-cell tolerance can be caused by systemical antigen application and subsequent presentation by non-professional APCs lacking costimulatory signals (187). In addition, changes regarding the administration of peptides have shown to be crucial for the immune response, either leading to T-cell induction or rendering T cells unresponsive. These changes imply the amount of antigen, route and frequency of application and the used adjuvant (188). Another critical factor with effect on the immune response are the peptide's chemical properties: Amphiphilic epitopes have proven higher

immunogenicity than their non-amphiphilic counterparts (189, 190). Due to mentioned factors, peptide-based vaccines have to be employed with caution in a human setting (68).

5.1 Impact of T-cell subsets and differentiation in ATT

T cells undergo differentiation, comprising the following subsets in their development: naïve, stem cell memory (SCM), central memory (CM), effector memory (EM) and finally effector cells. Although later phenotypes are associated with increased production of target-eliminating molecules like granzymes and IFN- γ , proliferation potential and antitumor efficacy declines along the differentiation process (191). Accordingly, CD8⁺ cells have shown to decrease in survival and proliferation capacity the more they are stimulated with IL-2 and their specific antigen (43). This paradox might be explained by the loss of the ability to produce IL-2, to home to lymph nodes and to resist apoptotic death along the differentiation process (43). Sommermeyer *et al.* showed that T-cell subsets as well as differentiation have an impact on antitumor effect in CD19-directed CAR T-cell therapy (192): When targeting disseminated lymphoma in murine models, superior efficacy among CD4⁺ cells was observed in samples derived from naïve and CM subsets. Using CD8⁺ cells in the same model, the strongest antitumor efficacy was detected in CM cell-derived samples. In the same study examining CAR T cells they concluded that CD4⁺ T cells support enhanced CD8⁺ T-cell proliferation. Notably, the combination of CD8⁺ CM-derived cells with CD4⁺ cells from either the naïve or CM subset conferred the strongest antitumor activity (95).

In the present project, phenotyping of the T cells was included in final ICS measurement, reflecting T-cell differentiation after seven restimulations. Surface markers CD45RO and CD62L (L-selectin) were measured to assess phenotypes. Using this panel, distinction between naïve and SCM T cells is not possible. When comparing T cells that induced a peptide-specific response (Tpos), and those that did not (Tneg), naïve/SCM cell proportion was the only one significantly different: naïve/SCM cells averaged 23.03 % in Tpos compared to 15.32 % in Tneg. Moreover, positive control in final ICS measurement was realized by PMA/Ionomycin flow-cytometric stain. Naïve/SCM and CM cell proportion combined amounted to 7.12 %, implying a down-regulation of L-selectin during 14 hours of stimulation, which is consistent with its properties: L-selectin is a cell adhesion molecule on leukocytes, responsible for their homing to lymph nodes and migration to inflammation sites (193, 194). This is mediated through tethering and rolling of the leukocytes on the endothelium. Upon activation, L-selectin is rapidly shed from the surface of leukocytes (195). Down-regulation of L-selectin is also induced by chemoattractants such as PMA (196).

6 Conclusion and outlook

In conclusion, we have demonstrated in a “proof a concept” approach with pediatric medulloblastoma that immunogenicity of tumor-specific neoantigens can be detected even against tumors with low mutational burden. Identification of neoantigens was accomplished through DNA and RNA sequencing

technologies and computational affinity prediction. Mutation-specific T-cell responses were determined *via* flow-cytometric measurement of IFN- γ and TNF- α and were found against 9/19 mutant peptides.

In this project, unbiased PBMC-derived DCs and PBLs from healthy donors were used. Strønen *et al* found that such naïve T cells can specifically respond to neoepitopes that had been neglected by autologous patient T cells (49). Further trials including patient T cells would be useful to examine to what extent they are reactive to tumor-specific neoepitopes. Those cells are often impaired and driven to exhaustion as a result of constant tumor-mediated inflammatory setting and antigen exposure (197). However, autologous TILs can mediate durable responses in patients with metastatic melanoma (174).

Mutated tumor-specific epitopes are a promising target for immunotherapy: As they have not undergone central tolerance mechanisms they are prone to be recognized as non-self antigens. Due to their exclusive expression on the tumor, risk for autoimmunity is reduced. Identification of immunogenic neoantigens paves the path for personalized therapeutic strategies such as peptide vaccination and adoptive T-cell transfer in pediatric patients with advanced medulloblastoma.

E Summary

Medulloblastoma is the most common malignant brain tumor in childhood and adolescence and constitutes an important cause for cancer-related death in pediatric patients. Although standard therapy including surgery, chemotherapy and radiation can cure up to 80 % of average-risk patients, they imply severe cognitive long-term adverse effects and are unsatisfactory in advanced tumors. Therefore, alternative treatment strategies need to be established. Immunotherapeutic approaches like peptide vaccination and adoptive T-cell transfer (ATT) aim at enhancing self-protection through detection and elimination of malignant cells. Tumor-specific neoepitopes are promising targets for ATT as they are expressed exclusively by cancer tissue. Moreover, administration of mutation-derived peptide vaccines allows augmenting the endogenous immune response through abundant presentation of tumor antigen. In this proof-of-concept study we demonstrate a highly individualized approach where patient-specific neoepitopes are determined and tested for immunogenicity.

Primary tumor samples from two pediatric medulloblastoma patients were analyzed in this project. Tumor-specific mutations were identified by next generation sequencing of tumor tissue and whole blood. Variants were confirmed by deep sequencing. In order to identify neoepitope peptides presented by the patients' human leucocyte antigen (HLA) molecules, HLA binding affinity was predicted *in silico* by netMHC database. Respective peptides were synthesized and blood cells from healthy donors matching the patients' HLA types were used to provide T lymphocytes and dendritic cells for antigen presentation. After seven restimulations *in vitro*, CD8⁺ cytotoxic T-cell reactivity against neoepitopes was assessed *via* flow-cytometric analysis of Interferon gamma and Tumor Necrosis Factor alpha release. A successful *de novo* T-cell response was induced for 9 of 19 tested peptides.

In this proof-of-principle study we show that induction of a T-cell response against medulloblastoma-derived neoantigens is feasible despite low mutational burden and low immunogenicity. In the future, this strategy can be used to synthesize individualized peptide cocktails for peptide vaccination or identify medulloblastoma-specific T-cell receptors for ATT. Long-term aims of this study are the identification of medulloblastoma/T-cell interaction and improvement of current treatment options for pediatric patients with advanced medulloblastoma.

E Zusammenfassung

Medulloblastom ist der häufigste bösartige Hirntumor im Kindes- und Jugendalter und bedeutend beteiligt an krebsassoziierten Todesfällen in pädiatrischen Patienten. Obwohl Standardtherapien, bestehend aus Operation, Chemotherapie und Bestrahlung, bis zu 80 % der Patienten mit durchschnittlichem Risiko heilen können, verursachen sie schwere kognitive Langzeitfolgen und wirken in fortgeschrittenen Tumorstadien unbefriedigend. Daher müssen alternative Behandlungsstrategien etabliert werden. Immuntherapeutische Ansätze wie Peptidvakzinierung und adoptiver T-Zell-Transfer (ATT) zielen darauf ab, die Mittel des Körpers zur Erkennung und Elimination von malignen Zellen zu steigern. Tumorspezifische Neoepitope sind vielversprechende Targets für ATT, da sie ausschließlich vom Tumorgewebe exprimiert werden. Weiterhin erlaubt die Verabreichung von mutationsbasierten Peptidvakzinen eine Zunahme der endogenen Immunantwort durch vielfache Tumorantigen-Präsentation. In dieser Machbarkeitsstudie zeigen wir eine vollkommen individualisierte Vorgehensweise, mit der patientenspezifische Neoepitope ermittelt und auf Immunogenität getestet werden.

Primärtumor-Proben von zwei pädiatrischen Medulloblastom-Patienten wurden in diesem Projekt eingesetzt. Tumorspezifische Mutationen wurden durch Next Generation Sequencing von Tumorgewebe und Blutzellen identifiziert. Die Varianten wurden durch Deep Sequencing bestätigt. Um Neoepitope zu ermitteln, deren Präsentation durch die humanen Leukozytenantigen-Moleküle (HLA) der Patienten angenommen werden konnte, wurde die HLA-Bindungsaffinität durch die netMHC-Datenbank *in silico* vorausgesagt und die so bestimmten Peptide synthetisiert. Blutzellen von gesunden Spendern, deren HLA-Typen denen der Patienten entsprachen, wurden für die Bereitstellung von T-Lymphozyten und dendritischen Zellen zur Antigenpräsentation verwendet. Nach sieben Restimulationen *in vitro* wurde die Reaktivität von zytotoxischen CD8⁺ T-Zellen gegen die Neoepitope anhand der durchflusszytometrisch bestimmten Ausschüttung von Interferon-gamma und Tumornekrosefaktor-alpha untersucht. Eine erfolgreiche *de novo* T-Zell-Antwort wurde für 9 von 19 getesteten Peptiden induziert.

In dieser Machbarkeitsstudie zeigen wir, dass die Induktion einer T-Zell-Antwort gegen Medulloblastom-assoziierte Neoepitope trotz niedriger Mutationslast und Immunogenität möglich ist. Zukünftig kann dieser Ansatz genutzt werden, um individualisierte Peptidcocktails für Peptidvakzinierung herzustellen oder Medulloblastom-spezifische T-Zell-Rezeptoren für ATT zu ermitteln. Langfristige Ziele dieser Studie sind die Bestimmung der Medulloblastom/T-Zell-Interaktion und die Verbesserung der aktuellen Behandlungsoptionen für pädiatrische Patienten mit fortgeschrittenem Medulloblastom.

F References

1. Hanahan D, Weinberg RA. Hallmarks of cancer: the next generation. *Cell*. 2011;144(5):646-74.
2. Parkin J, Cohen B. An overview of the immune system. *Lancet*. 2001;357(9270):1777-89.
3. Strutt TM, McKinstry KK, Dibble JP, Winchell C, Kuang Y, Curtis JD, et al. Memory CD4+ T cells induce innate responses independently of pathogen. *Nat Med*. 2010;16(5):558-64, 1p following 64.
4. Schwartz MA, Kolhatkar NS, Thouvenel C, Khim S, Rawlings DJ. CD4+ T cells and CD40 participate in selection and homeostasis of peripheral B cells. *J Immunol*. 2014;193(7):3492-502.
5. Beuneu H, Garcia Z, Bousso P. Cutting edge: cognate CD4 help promotes recruitment of antigen-specific CD8 T cells around dendritic cells. *J Immunol*. 2006;177(3):1406-10.
6. Luckheeram RV, Zhou R, Verma AD, Xia B. CD4(+)-T cells: differentiation and functions. *Clin Dev Immunol*. 2012;2012:925135.
7. Hewitt EW. The MHC class I antigen presentation pathway: strategies for viral immune evasion. *Immunology*. 2003;110(2):163-9.
8. Ting JP, Trowsdale J. Genetic control of MHC class II expression. *Cell*. 2002;109 Suppl:S21-33.
9. Rammensee HG, Falk K, Rotzschke O. Peptides naturally presented by MHC class I molecules. *Annu Rev Immunol*. 1993;11:213-44.
10. Bouvier M, Wiley DC. Importance of peptide amino and carboxyl termini to the stability of MHC class I molecules. *Science*. 1994;265(5170):398-402.
11. Rammensee HG, Friede T, Stevanović S. MHC ligands and peptide motifs: first listing. *Immunogenetics*. 1995;41(4):178-228.
12. Lurquin C, Van Pel A, Mariame B, De Plaen E, Szikora JP, Janssens C, et al. Structure of the gene of tum- transplantation antigen P91A: the mutated exon encodes a peptide recognized with Ld by cytolytic T cells. *Cell*. 1989;58(2):293-303.
13. Kawashima I, Tsai V, Southwood S, Takesako K, Sette A, Celis E. Identification of HLA-A3-restricted cytotoxic T lymphocyte epitopes from carcinoembryonic antigen and HER-2/neu by primary in vitro immunization with peptide-pulsed dendritic cells. *Cancer Res*. 1999;59(2):431-5.
14. Weinzierl AO, Maurer D, Altenberend F, Schneiderhan-Marra N, Klingel K, Schoor O, et al. A cryptic vascular endothelial growth factor T-cell epitope: identification and characterization by mass spectrometry and T-cell assays. *Cancer Res*. 2008;68(7):2447-54.
15. Kang X, Kawakami Y, el-Gamil M, Wang R, Sakaguchi K, Yannelli JR, et al. Identification of a tyrosinase epitope recognized by HLA-A24-restricted, tumor-infiltrating lymphocytes. *J Immunol*. 1995;155(3):1343-8.
16. Gold P, Freedman SO. Demonstration of Tumor-Specific Antigens in Human Colonic Carcinomata by Immunological Tolerance and Absorption Techniques. *J Exp Med*. 1965;121:439-62.
17. Coulie PG, Brichard V, Van Pel A, Wolfel T, Schneider J, Traversari C, et al. A new gene coding for a differentiation antigen recognized by autologous cytolytic T lymphocytes on HLA-A2 melanomas. *J Exp Med*. 1994;180(1):35-42.
18. Brentjens RJ, Riviere I, Park JH, Davila ML, Wang X, Stefanski J, et al. Safety and persistence of adoptively transferred autologous CD19-targeted T cells in patients with relapsed or chemotherapy refractory B-cell leukemias. *Blood*. 2011;118(18):4817-28.
19. Maude SL, Teachey DT, Porter DL, Grupp SA. CD19-targeted chimeric antigen receptor T-cell therapy for acute lymphoblastic leukemia. *Blood*. 2015;125(26):4017-23.
20. Parkhurst MR, Yang JC, Langan RC, Dudley ME, Nathan DA, Feldman SA, et al. T cells targeting carcinoembryonic antigen can mediate regression of metastatic colorectal cancer but induce severe transient colitis. *Mol Ther*. 2011;19(3):620-6.
21. Akers SN, Odunsi K, Karpf AR. Regulation of cancer germline antigen gene expression: implications for cancer immunotherapy. *Future Oncol*. 2010;6(5):717-32.
22. Sang M, Lian Y, Zhou X, Shan B. MAGE-A family: attractive targets for cancer immunotherapy. *Vaccine*. 2011;29(47):8496-500.
23. Coulie PG, Van den Eynde BJ, van der Bruggen P, Boon T. Tumour antigens recognized by T lymphocytes: at the core of cancer immunotherapy. *Nat Rev Cancer*. 2014;14(2):135-46.

24. Vigneron N. Human Tumor Antigens and Cancer Immunotherapy. *BioMed research international*. 2015;2015:948501.
25. Schietinger A, Philip M, Schreiber H. Specificity in cancer immunotherapy. *Seminars in immunology*. 2008;20(5):276-85.
26. Gjertsen MK, Bjorheim J, Saeterdal I, Myklebust J, Gaudernack G. Cytotoxic CD4+ and CD8+ T lymphocytes, generated by mutant p21-ras (12Val) peptide vaccination of a patient, recognize 12Val-dependent nested epitopes present within the vaccine peptide and kill autologous tumour cells carrying this mutation. *Int J Cancer*. 1997;72(5):784-90.
27. Leisegang M, Engels B, Schreiber K, Yew PY, Kiyotani K, Idel C, et al. Eradication of Large Solid Tumors by Gene Therapy with a T-Cell Receptor Targeting a Single Cancer-Specific Point Mutation. *Clin Cancer Res*. 2016;22(11):2734-43.
28. Roberts SA, Gordenin DA. Hypermutation in human cancer genomes: footprints and mechanisms. *Nat Rev Cancer*. 2014;14(12):786-800.
29. Alexandrov LB, Nik-Zainal S, Wedge DC, Aparicio SA, Behjati S, Biankin AV, et al. Signatures of mutational processes in human cancer. *Nature*. 2013;500(7463):415-21.
30. Tran E, Turcotte S, Gros A, Robbins PF, Lu YC, Dudley ME, et al. Cancer immunotherapy based on mutation-specific CD4+ T cells in a patient with epithelial cancer. *Science*. 2014;344(6184):641-5.
31. Swann JB, Smyth MJ. Immune surveillance of tumors. *J Clin Invest*. 2007;117(5):1137-46.
32. Tran E, Ahmadzadeh M, Lu YC, Gros A, Turcotte S, Robbins PF, et al. Immunogenicity of somatic mutations in human gastrointestinal cancers. *Science*. 2015;350(6266):1387-90.
33. Kim R, Emi M, Tanabe K. Cancer immunoediting from immune surveillance to immune escape. *Immunology*. 2007;121(1):1-14.
34. Ehrlich P. Über den jetzigen Stand der Karzinomforschung. Beiträge zur experimentellen Pathologie und Chemotherapie. 1909:117-64.
35. Ehrlich P. The Collected Papers of Paul Ehrlich. *Journal of the Royal Society of Medicine*. 1957;50.
36. Burnet M. Cancer: a biological approach. III. Viruses associated with neoplastic conditions. IV. Practical applications. *Br Med J*. 1957;1(5023):841-7.
37. Clark WH, Jr., Elder DE, Guerry Dt, Braitman LE, Trock BJ, Schultz D, et al. Model predicting survival in stage I melanoma based on tumor progression. *J Natl Cancer Inst*. 1989;81(24):1893-904.
38. Zhang L, Conejo-Garcia JR, Katsaros D, Gimotty PA, Massobrio M, Regnani G, et al. Intratumoral T cells, recurrence, and survival in epithelial ovarian cancer. *N Engl J Med*. 2003;348(3):203-13.
39. Ishigami S, Natsugoe S, Tokuda K, Nakajo A, Che X, Iwashige H, et al. Prognostic value of intratumoral natural killer cells in gastric carcinoma. *Cancer*. 2000;88(3):577-83.
40. Villegas FR, Coca S, Villarrubia VG, Jimenez R, Chillon MJ, Jareno J, et al. Prognostic significance of tumor infiltrating natural killer cells subset CD57 in patients with squamous cell lung cancer. *Lung Cancer*. 2002;35(1):23-8.
41. Coca S, Perez-Piqueras J, Martinez D, Colmenarejo A, Saez MA, Vallejo C, et al. The prognostic significance of intratumoral natural killer cells in patients with colorectal carcinoma. *Cancer*. 1997;79(12):2320-8.
42. Smyth MJ, Thia KY, Street SE, MacGregor D, Godfrey DI, Trapani JA. Perforin-mediated cytotoxicity is critical for surveillance of spontaneous lymphoma. *J Exp Med*. 2000;192(5):755-60.
43. Restifo NP, Dudley ME, Rosenberg SA. Adoptive immunotherapy for cancer: harnessing the T cell response. *Nat Rev Immunol*. 2012;12(4):269-81.
44. Dighe AS, Richards E, Old LJ, Schreiber RD. Enhanced in vivo growth and resistance to rejection of tumor cells expressing dominant negative IFN gamma receptors. *Immunity*. 1994;1(6):447-56.
45. Kaplan DH, Shankaran V, Dighe AS, Stockert E, Aguet M, Old LJ, et al. Demonstration of an interferon gamma-dependent tumor surveillance system in immunocompetent mice. *Proc Natl Acad Sci U S A*. 1998;95(13):7556-61.
46. Street SE, Cretney E, Smyth MJ. Perforin and interferon-gamma activities independently control tumor initiation, growth, and metastasis. *Blood*. 2001;97(1):192-7.
47. Dunn GP, Old LJ, Schreiber RD. The three Es of cancer immunoediting. *Annu Rev Immunol*. 2004;22:329-60.

48. von Bernstorff W, Voss M, Freichel S, Schmid A, Vogel I, Johnk C, et al. Systemic and local immunosuppression in pancreatic cancer patients. *Clin Cancer Res*. 2001;7(3 Suppl):925s-32s.
49. Stronen E, Toebes M, Kelderman S, van Buuren MM, Yang W, van Rooij N, et al. Targeting of cancer neoantigens with donor-derived T cell receptor repertoires. *Science*. 2016;352(6291):1337-41.
50. Radoja S, Rao TD, Hillman D, Frey AB. Mice bearing late-stage tumors have normal functional systemic T cell responses in vitro and in vivo. *J Immunol*. 2000;164(5):2619-28.
51. Azuma T, Yao S, Zhu G, Flies AS, Flies SJ, Chen L. B7-H1 is a ubiquitous antiapoptotic receptor on cancer cells. *Blood*. 2008;111(7):3635-43.
52. Juneja VR, McGuire KA, Manguso RT, LaFleur MW, Collins N, Haining WN, et al. PD-L1 on tumor cells is sufficient for immune evasion in immunogenic tumors and inhibits CD8 T cell cytotoxicity. *J Exp Med*. 2017;214(4):895-904.
53. Lau J, Cheung J, Navarro A, Lianoglou S, Haley B, Totpal K, et al. Tumour and host cell PD-L1 is required to mediate suppression of anti-tumour immunity in mice. *Nat Commun*. 2017;8:14572.
54. Kataoka T, Schroter M, Hahne M, Schneider P, Irmeler M, Thome M, et al. FLIP prevents apoptosis induced by death receptors but not by perforin/granzyme B, chemotherapeutic drugs, and gamma irradiation. *J Immunol*. 1998;161(8):3936-42.
55. Huber V, Fais S, Iero M, Lugini L, Canese P, Squarcina P, et al. Human colorectal cancer cells induce T-cell death through release of proapoptotic microvesicles: role in immune escape. *Gastroenterology*. 2005;128(7):1796-804.
56. Gabrilovich D, Ishida T, Oyama T, Ran S, Kravtsov V, Nadaf S, et al. Vascular endothelial growth factor inhibits the development of dendritic cells and dramatically affects the differentiation of multiple hematopoietic lineages in vivo. *Blood*. 1998;92(11):4150-66.
57. Kim R, Emi M, Tanabe K. Cancer cell immune escape and tumor progression by exploitation of anti-inflammatory and pro-inflammatory responses. *Cancer Biol Ther*. 2005;4(9):924-33.
58. Campoli M, Chang CC, Ferrone S. HLA class I antigen loss, tumor immune escape and immune selection. *Vaccine*. 2002;20 Suppl 4:A40-5.
59. Raghavan S, Quiding-Jarbrink M. Regulatory T cells in gastrointestinal tumors. *Expert Rev Gastroenterol Hepatol*. 2011;5(4):489-501.
60. Ventola CL. Cancer Immunotherapy, Part 1: Current Strategies and Agents. *P T*. 2017;42(6):375-83.
61. Tan SY, Grimes S. Paul Ehrlich (1854-1915): man with the magic bullet. *Singapore Med J*. 2010;51(11):842-3.
62. Pardoll DM. The blockade of immune checkpoints in cancer immunotherapy. *Nat Rev Cancer*. 2012;12(4):252-64.
63. Topalian SL, Drake CG, Pardoll DM. Immune checkpoint blockade: a common denominator approach to cancer therapy. *Cancer Cell*. 2015;27(4):450-61.
64. Davis KL, Agarwal AM, Verma AR. Checkpoint inhibition in pediatric hematologic malignancies. *Pediatr Hematol Oncol*. 2017;34(6-7):379-94.
65. Topp MS, Kufer P, Gokbuget N, Goebeler M, Klinger M, Neumann S, et al. Targeted therapy with the T-cell-engaging antibody blinatumomab of chemotherapy-refractory minimal residual disease in B-lineage acute lymphoblastic leukemia patients results in high response rate and prolonged leukemia-free survival. *J Clin Oncol*. 2011;29(18):2493-8.
66. Alatrash G, Jakher H, Stafford PD, Mittendorf EA. Cancer immunotherapies, their safety and toxicity. *Expert Opin Drug Saf*. 2013;12(5):631-45.
67. Slingluff CL, Jr. The present and future of peptide vaccines for cancer: single or multiple, long or short, alone or in combination? *Cancer J*. 2011;17(5):343-50.
68. Toes RE, Offringa R, Blom RJ, Melief CJ, Kast WM. Peptide vaccination can lead to enhanced tumor growth through specific T-cell tolerance induction. *Proc Natl Acad Sci U S A*. 1996;93(15):7855-60.
69. Slingluff CL, Jr., Petroni GR, Olson W, Czarkowski A, Grosh WW, Smolkin M, et al. Helper T-cell responses and clinical activity of a melanoma vaccine with multiple peptides from MAGE and melanocytic differentiation antigens. *J Clin Oncol*. 2008;26(30):4973-80.
70. Schwartzenuber DJ, Lawson DH, Richards JM, Conry RM, Miller DM, Treisman J, et al. gp100 peptide vaccine and interleukin-2 in patients with advanced melanoma. *N Engl J Med*. 2011;364(22):2119-27.

71. Mittendorf EA, Clifton GT, Holmes JP, Clive KS, Patil R, Benavides LC, et al. Clinical trial results of the HER-2/neu (E75) vaccine to prevent breast cancer recurrence in high-risk patients: from US Military Cancer Institute Clinical Trials Group Study I-01 and I-02. *Cancer*. 2012;118(10):2594-602.
72. Kotsakis A, Papadimitraki E, Vetsika EK, Aggouraki D, Dermitzaki EK, Hatzidaki D, et al. A phase II trial evaluating the clinical and immunologic response of HLA-A2(+) non-small cell lung cancer patients vaccinated with an hTERT cryptic peptide. *Lung Cancer*. 2014;86(1):59-66.
73. Suzuki N, Hazama S, Iguchi H, Uesugi K, Tanaka H, Hirakawa K, et al. Phase II clinical trial of peptide cocktail therapy for patients with advanced pancreatic cancer: VENUS-PC study. *Cancer Sci*. 2017;108(1):73-80.
74. Iinuma H, Fukushima R, Inaba T, Tamura J, Inoue T, Ogawa E, et al. Phase I clinical study of multiple epitope peptide vaccine combined with chemoradiation therapy in esophageal cancer patients. *J Transl Med*. 2014;12:84.
75. Fujiwara Y, Okada K, Omori T, Sugimura K, Miyata H, Ohue M, et al. Multiple therapeutic peptide vaccines for patients with advanced gastric cancer. *Int J Oncol*. 2017;50(5):1655-62.
76. Schuler PJ, Harasymczuk M, Visus C, Deleo A, Trivedi S, Lei Y, et al. Phase I dendritic cell p53 peptide vaccine for head and neck cancer. *Clin Cancer Res*. 2014;20(9):2433-44.
77. Rosenberg SA, Packard BS, Aebersold PM, Solomon D, Topalian SL, Toy ST, et al. Use of tumor-infiltrating lymphocytes and interleukin-2 in the immunotherapy of patients with metastatic melanoma. A preliminary report. *N Engl J Med*. 1988;319(25):1676-80.
78. Dudley ME, Wunderlich JR, Robbins PF, Yang JC, Hwu P, Schwartzentruber DJ, et al. Cancer regression and autoimmunity in patients after clonal repopulation with antitumor lymphocytes. *Science*. 2002;298(5594):850-4.
79. Rosenberg SA, Restifo NP. Adoptive cell transfer as personalized immunotherapy for human cancer. *Science*. 2015;348(6230):62-8.
80. Merhavi-Shoham E, Itzhaki O, Markel G, Schachter J, Besser MJ. Adoptive Cell Therapy for Metastatic Melanoma. *Cancer J*. 2017;23(1):48-53.
81. Jochems C, Schlom J. Tumor-infiltrating immune cells and prognosis: the potential link between conventional cancer therapy and immunity. *Exp Biol Med (Maywood)*. 2011;236(5):567-79.
82. Rivoltini L, Arienti F, Orazi A, Cefalo G, Gasparini M, Gambacorti-Passerini C, et al. Phenotypic and functional analysis of lymphocytes infiltrating paediatric tumours, with a characterization of the tumour phenotype. *Cancer Immunol Immunother*. 1992;34(4):241-51.
83. Barrett DM, Grupp SA, June CH. Chimeric Antigen Receptor- and TCR-Modified T Cells Enter Main Street and Wall Street. *J Immunol*. 2015;195(3):755-61.
84. Sadelain M, Brentjens R, Riviere I. The basic principles of chimeric antigen receptor design. *Cancer discovery*. 2013;3(4):388-98.
85. Yang S, Rosenberg SA, Morgan RA. Clinical-scale lentiviral vector transduction of PBL for TCR gene therapy and potential for expression in less-differentiated cells. *J Immunother*. 2008;31(9):830-9.
86. Morgan RA, Dudley ME, Wunderlich JR, Hughes MS, Yang JC, Sherry RM, et al. Cancer regression in patients after transfer of genetically engineered lymphocytes. *Science*. 2006;314(5796):126-9.
87. Sadelain M, Brentjens R, Riviere I. The promise and potential pitfalls of chimeric antigen receptors. *Curr Opin Immunol*. 2009;21(2):215-23.
88. Kochenderfer JN, Rosenberg SA. Treating B-cell cancer with T cells expressing anti-CD19 chimeric antigen receptors. *Nat Rev Clin Oncol*. 2013;10(5):267-76.
89. Kochenderfer JN, Dudley ME, Kassim SH, Somerville RP, Carpenter RO, Stetler-Stevenson M, et al. Chemotherapy-refractory diffuse large B-cell lymphoma and indolent B-cell malignancies can be effectively treated with autologous T cells expressing an anti-CD19 chimeric antigen receptor. *J Clin Oncol*. 2015;33(6):540-9.
90. Firor AE, Jares A, Ma Y. From humble beginnings to success in the clinic: Chimeric antigen receptor-modified T-cells and implications for immunotherapy. *Exp Biol Med (Maywood)*. 2015;240(8):1087-98.
91. Johnson LA, Morgan RA, Dudley ME, Cassard L, Yang JC, Hughes MS, et al. Gene therapy with human and mouse T-cell receptors mediates cancer regression and targets normal tissues expressing cognate antigen. *Blood*. 2009;114(3):535-46.

92. Cameron BJ, Gerry AB, Dukes J, Harper JV, Kannan V, Bianchi FC, et al. Identification of a Titin-derived HLA-A1-presented peptide as a cross-reactive target for engineered MAGE A3-directed T cells. *Sci Transl Med*. 2013;5(197):197ra03.
93. Linette GP, Stadtmauer EA, Maus MV, Rapoport AP, Levine BL, Emery L, et al. Cardiovascular toxicity and titin cross-reactivity of affinity-enhanced T cells in myeloma and melanoma. *Blood*. 2013;122(6):863-71.
94. Morgan RA, Chinnasamy N, Abate-Daga D, Gros A, Robbins PF, Zheng Z, et al. Cancer regression and neurological toxicity following anti-MAGE-A3 TCR gene therapy. *J Immunother*. 2013;36(2):133-51.
95. Arora RS, Alston RD, Eden TO, Estlin EJ, Moran A, Birch JM. Age-incidence patterns of primary CNS tumors in children, adolescents, and adults in England. *Neuro Oncol*. 2009;11(4):403-13.
96. Buckner JC, Brown PD, O'Neill BP, Meyer FB, Wetmore CJ, Uhm JH. Central nervous system tumors. *Mayo Clin Proc*. 2007;82(10):1271-86.
97. Fogarty MP, Kessler JD, Wechsler-Reya RJ. Morphing into cancer: the role of developmental signaling pathways in brain tumor formation. *J Neurobiol*. 2005;64(4):458-75.
98. Alston RD, Newton R, Kelsey A, Newbould MJ, Birch JM, Lawson B, et al. Childhood medulloblastoma in northwest England 1954 to 1997: incidence and survival. *Dev Med Child Neurol*. 2003;45(5):308-14.
99. Louis DN, Perry A, Reifenberger G, von Deimling A, Figarella-Branger D, Cavenee WK, et al. The 2016 World Health Organization Classification of Tumors of the Central Nervous System: a summary. *Acta Neuropathol*. 2016;131(6):803-20.
100. Roussel MF, Hatten ME. Cerebellum development and medulloblastoma. *Curr Top Dev Biol*. 2011;94:235-82.
101. Phoenix TN, Patmore DM, Boop S, Boulos N, Jacus MO, Patel YT, et al. Medulloblastoma Genotype Dictates Blood Brain Barrier Phenotype. *Cancer Cell*. 2016;29(4):508-22.
102. Ellison DW, Dalton J, Kocak M, Nicholson SL, Fraga C, Neale G, et al. Medulloblastoma: clinicopathological correlates of SHH, WNT, and non-SHH/WNT molecular subgroups. *Acta Neuropathol*. 2011;121(3):381-96.
103. Louis DN, Ohgaki H, Wiestler OD, Cavenee WK, Burger PC, Jouvet A, et al. The 2007 WHO classification of tumours of the central nervous system. *Acta Neuropathol*. 2007;114(2):97-109.
104. Jones DT, Jager N, Kool M, Zichner T, Hutter B, Sultan M, et al. Dissecting the genomic complexity underlying medulloblastoma. *Nature*. 2012;488(7409):100-5.
105. Robinson G, Parker M, Kranenburg TA, Lu C, Chen X, Ding L, et al. Novel mutations target distinct subgroups of medulloblastoma. *Nature*. 2012;488(7409):43-8.
106. Pugh TJ, Weeraratne SD, Archer TC, Pomeranz Krummel DA, Auclair D, Bochicchio J, et al. Medulloblastoma exome sequencing uncovers subtype-specific somatic mutations. *Nature*. 2012;488(7409):106-10.
107. Archer TC, Pomeroy SL. Medulloblastoma biology in the post-genomic era. *Future Oncol*. 2012;8(12):1597-604.
108. Northcott PA, Buchhalter I, Morrissy AS, Hovestadt V, Weischenfeldt J, Ehrenberger T, et al. The whole-genome landscape of medulloblastoma subtypes. *Nature*. 2017;547(7663):311-7.
109. Rutkowski S, von Hoff K, Emser A, Zwiener I, Pietsch T, Figarella-Branger D, et al. Survival and prognostic factors of early childhood medulloblastoma: an international meta-analysis. *J Clin Oncol*. 2010;28(33):4961-8.
110. Gajjar A, Chintagumpala M, Ashley D, Kellie S, Kun LE, Merchant TE, et al. Risk-adapted craniospinal radiotherapy followed by high-dose chemotherapy and stem-cell rescue in children with newly diagnosed medulloblastoma (St Jude Medulloblastoma-96): long-term results from a prospective, multicentre trial. *Lancet Oncol*. 2006;7(10):813-20.
111. Mabbott DJ, Penkman L, Witol A, Strother D, Bouffet E. Core neurocognitive functions in children treated for posterior fossa tumors. *Neuropsychology*. 2008;22(2):159-68.
112. Sabel M, Fleischhack G, Tippelt S, Gustafsson G, Doz F, Kortmann R, et al. Relapse patterns and outcome after relapse in standard risk medulloblastoma: a report from the HIT-SIOP-PNET4 study. *J Neurooncol*. 2016;129(3):515-24.

113. Hill RM, Kuijper S, Lindsey JC, Petrie K, Schwalbe EC, Barker K, et al. Combined MYC and P53 defects emerge at medulloblastoma relapse and define rapidly progressive, therapeutically targetable disease. *Cancer Cell*. 2015;27(1):72-84.
114. Koschmann C, Bloom K, Upadhyaya S, Geyer JR, Leary SE. Survival After Relapse of Medulloblastoma. *J Pediatr Hematol Oncol*. 2016;38(4):269-73.
115. Rammensee H, Bachmann J, Emmerich NP, Bachor OA, Stevanovic S. SYFPEITHI: database for MHC ligands and peptide motifs. *Immunogenetics*. 1999;50(3-4):213-9.
116. Blaeschke F, Paul MC, Schuhmann MU, Rabsteyn A, Schroeder C, Casadei N, et al. Low mutational load in pediatric medulloblastoma still translates into neoantigens as targets for specific T-cell immunotherapy. *Cytotherapy*. 2019;21(9):973-86.
117. Dhall G. Medulloblastoma. *J Child Neurol*. 2009;24(11):1418-30.
118. Boon T, van der Bruggen P. Human tumor antigens recognized by T lymphocytes. *J Exp Med*. 1996;183(3):725-9.
119. Cohen CJ, Gartner JJ, Horovitz-Fried M, Shamalov K, Trebska-McGowan K, Bliskovsky VV, et al. Isolation of neoantigen-specific T cells from tumor and peripheral lymphocytes. *J Clin Invest*. 2015;125(10):3981-91.
120. Popovic J, Li LP, Kloetzel PM, Leisegang M, Uckert W, Blankenstein T. The only proposed T-cell epitope derived from the TEL-AML1 translocation is not naturally processed. *Blood*. 2011;118(4):946-54.
121. Parker KC, Shields M, DiBrino M, Brooks A, Coligan JE. Peptide binding to MHC class I molecules: implications for antigenic peptide prediction. *Immunol Res*. 1995;14(1):34-57.
122. Matsushita H, Vesely MD, Koboldt DC, Rickert CG, Uppaluri R, Magrini VJ, et al. Cancer exome analysis reveals a T-cell-dependent mechanism of cancer immunoediting. *Nature*. 2012;482(7385):400-4.
123. Robbins PF, Lu YC, El-Gamil M, Li YF, Gross C, Gartner J, et al. Mining exomic sequencing data to identify mutated antigens recognized by adoptively transferred tumor-reactive T cells. *Nat Med*. 2013;19(6):747-52.
124. Schreiber H, Rowley JD, Rowley DA. Targeting mutations predictably. *Blood*. 2011;118(4):830-1.
125. Paul S, Weiskopf D, Angelo MA, Sidney J, Peters B, Sette A. HLA class I alleles are associated with peptide-binding repertoires of different size, affinity, and immunogenicity. *J Immunol*. 2013;191(12):5831-9.
126. Engels B, Engelhard VH, Sidney J, Sette A, Binder DC, Liu RB, et al. Relapse or eradication of cancer is predicted by peptide-major histocompatibility complex affinity. *Cancer Cell*. 2013;23(4):516-26.
127. Nielsen M, Andreatta M. NetMHCpan-3.0; improved prediction of binding to MHC class I molecules integrating information from multiple receptor and peptide length datasets. *Genome Med*. 2016;8(1):33.
128. Kreiter S, Vormehr M, van de Roemer N, Diken M, Lower M, Diekmann J, et al. Mutant MHC class II epitopes drive therapeutic immune responses to cancer. *Nature*. 2015;520(7549):692-6.
129. Schellens IM, Hoof I, Meiring HD, Spijkers SN, Poelen MC, van Gaans-van den Brink JA, et al. Comprehensive Analysis of the Naturally Processed Peptide Repertoire: Differences between HLA-A and B in the Immunopeptidome. *PLoS One*. 2015;10(9):e0136417.
130. Fruci D, Rovero P, Falasca G, Chersi A, Sorrentino R, Butler R, et al. Anchor residue motifs of HLA class-I-binding peptides analyzed by the direct binding of synthetic peptides to HLA class I alpha chains. *Hum Immunol*. 1993;38(3):187-92.
131. Khalili JS, Hanson RW, Szallasi Z. In silico prediction of tumor antigens derived from functional missense mutations of the cancer gene census. *Oncoimmunology*. 2012;1(8):1281-9.
132. Kambayashi T, Laufer TM. Atypical MHC class II-expressing antigen-presenting cells: can anything replace a dendritic cell? *Nat Rev Immunol*. 2014;14(11):719-30.
133. Albert ML, Pearce SF, Francisco LM, Sauter B, Roy P, Silverstein RL, et al. Immature dendritic cells phagocytose apoptotic cells via alphavbeta5 and CD36, and cross-present antigens to cytotoxic T lymphocytes. *J Exp Med*. 1998;188(7):1359-68.
134. Wakim LM, Waithman J, van Rooijen N, Heath WR, Carbone FR. Dendritic cell-induced memory T cell activation in nonlymphoid tissues. *Science*. 2008;319(5860):198-202.

135. Tang-Huau TL, Gueguen P, Goudot C, Durand M, Bohec M, Baulande S, et al. Human in vivo-generated monocyte-derived dendritic cells and macrophages cross-present antigens through a vacuolar pathway. *Nat Commun.* 2018;9(1):2570.
136. Kuhn S, Yang J, Ronchese F. Monocyte-Derived Dendritic Cells Are Essential for CD8(+) T Cell Activation and Antitumor Responses After Local Immunotherapy. *Front Immunol.* 2015;6:584.
137. Gabrilovich DI, Chen HL, Girgis KR, Cunningham HT, Meny GM, Nadaf S, et al. Production of vascular endothelial growth factor by human tumors inhibits the functional maturation of dendritic cells. *Nat Med.* 1996;2(10):1096-103.
138. Menetrier-Caux C, Montmain G, Dieu MC, Bain C, Favrot MC, Caux C, et al. Inhibition of the differentiation of dendritic cells from CD34(+) progenitors by tumor cells: role of interleukin-6 and macrophage colony-stimulating factor. *Blood.* 1998;92(12):4778-91.
139. Ahrends T, Spanjaard A, Pilzecker B, Babala N, Bovens A, Xiao Y, et al. CD4(+) T Cell Help Confers a Cytotoxic T Cell Effector Program Including Coinhibitory Receptor Downregulation and Increased Tissue Invasiveness. *Immunity.* 2017;47(5):848-61 e5.
140. Bevan MJ. Helping the CD8(+) T-cell response. *Nat Rev Immunol.* 2004;4(8):595-602.
141. Castellino F, Germain RN. Cooperation between CD4+ and CD8+ T cells: when, where, and how. *Annu Rev Immunol.* 2006;24:519-40.
142. Dudley ME, Wunderlich JR, Shelton TE, Even J, Rosenberg SA. Generation of tumor-infiltrating lymphocyte cultures for use in adoptive transfer therapy for melanoma patients. *J Immunother.* 2003;26(4):332-42.
143. Fridman WH, Pages F, Sautes-Fridman C, Galon J. The immune contexture in human tumours: impact on clinical outcome. *Nat Rev Cancer.* 2012;12(4):298-306.
144. Schoenberger SP, Toes RE, van der Voort EI, Offringa R, Melief CJ. T-cell help for cytotoxic T lymphocytes is mediated by CD40-CD40L interactions. *Nature.* 1998;393(6684):480-3.
145. Voest EE, Kenyon BM, O'Reilly MS, Truitt G, D'Amato RJ, Folkman J. Inhibition of angiogenesis in vivo by interleukin 12. *J Natl Cancer Inst.* 1995;87(8):581-6.
146. Sun JC, Bevan MJ. Defective CD8 T cell memory following acute infection without CD4 T cell help. *Science.* 2003;300(5617):339-42.
147. Shedlock DJ, Whitmire JK, Tan J, MacDonald AS, Ahmed R, Shen H. Role of CD4 T cell help and costimulation in CD8 T cell responses during *Listeria monocytogenes* infection. *J Immunol.* 2003;170(4):2053-63.
148. Muccioli M, Longstaff C, Benencia F. Absence of CD4 T-cell help provides a robust CD8 T-cell response while inducing effective memory in a preclinical model of melanoma. *Immunotherapy.* 2012;4(5):477-81.
149. Jensen KK, Andreatta M, Marcatili P, Buus S, Greenbaum JA, Yan Z, et al. Improved methods for predicting peptide binding affinity to MHC class II molecules. *Immunology.* 2018;154(3):394-406.
150. Nielsen M, Lund O, Buus S, Lundegaard C. MHC class II epitope predictive algorithms. *Immunology.* 2010;130(3):319-28.
151. Brown JH, Jardetzky TS, Gorga JC, Stern LJ, Urban RG, Strominger JL, et al. Pillars article: three-dimensional structure of the human class II histocompatibility antigen HLA-DR1. *Nature.* 1993. 364: 33-39. *J Immunol.* 2015;194(1):5-11.
152. Chalmers ZR, Connelly CF, Fabrizio D, Gay L, Ali SM, Ennis R, et al. Analysis of 100,000 human cancer genomes reveals the landscape of tumor mutational burden. *Genome Med.* 2017;9(1):34.
153. Chen L, Tanriover G, Yano H, Friedlander R, Louvi A, Gunel M. Apoptotic functions of PDCD10/CCM3, the gene mutated in cerebral cavernous malformation 3. *Stroke.* 2009;40(4):1474-81.
154. Lauenborg B, Kopp K, Krejsgaard T, Eriksen KW, Geisler C, Dabelsteen S, et al. Programmed cell death-10 enhances proliferation and protects malignant T cells from apoptosis. *APMIS.* 2010;118(10):719-28.
155. He Y, Zhang H, Yu L, Gunel M, Boggon TJ, Chen H, et al. Stabilization of VEGFR2 signaling by cerebral cavernous malformation 3 is critical for vascular development. *Sci Signal.* 2010;3(116):ra26.

156. Cigoli MS, Avemaria F, De Benedetti S, Gesu GP, Accorsi LG, Parmigiani S, et al. PDCD10 gene mutations in multiple cerebral cavernous malformations. *PLoS One*. 2014;9(10):e110438.
157. Cameron J, Holla OL, Ranheim T, Kulseth MA, Berge KE, Leren TP. Effect of mutations in the PCSK9 gene on the cell surface LDL receptors. *Hum Mol Genet*. 2006;15(9):1551-8.
158. Xu X, Cui Y, Cao L, Zhang Y, Yin Y, Hu X. PCSK9 regulates apoptosis in human lung adenocarcinoma A549 cells via endoplasmic reticulum stress and mitochondrial signaling pathways. *Exp Ther Med*. 2017;13(5):1993-9.
159. Mukohara T. PI3K mutations in breast cancer: prognostic and therapeutic implications. *Breast Cancer (Dove Med Press)*. 2015;7:111-23.
160. Scheffler M, Bos M, Gardizi M, Konig K, Michels S, Fassunke J, et al. PIK3CA mutations in non-small cell lung cancer (NSCLC): genetic heterogeneity, prognostic impact and incidence of prior malignancies. *Oncotarget*. 2015;6(2):1315-26.
161. Cathomas G. PIK3CA in Colorectal Cancer. *Front Oncol*. 2014;4:35.
162. Broderick DK, Di C, Parrett TJ, Samuels YR, Cummins JM, McLendon RE, et al. Mutations of PIK3CA in anaplastic oligodendrogliomas, high-grade astrocytomas, and medulloblastomas. *Cancer Res*. 2004;64(15):5048-50.
163. Guerreiro AS, Fattet S, Fischer B, Shalaby T, Jackson SP, Schoenwaelder SM, et al. Targeting the PI3K p110alpha isoform inhibits medulloblastoma proliferation, chemoresistance, and migration. *Clin Cancer Res*. 2008;14(21):6761-9.
164. Hevner RF. Brain overgrowth in disorders of RTK-PI3K-AKT signaling: a mosaic of malformations. *Semin Perinatol*. 2015;39(1):36-43.
165. Adams HH, Hibar DP, Chouraki V, Stein JL, Nyquist PA, Renteria ME, et al. Novel genetic loci underlying human intracranial volume identified through genome-wide association. *Nat Neurosci*. 2016;19(12):1569-82.
166. Miller TW, Rexer BN, Garrett JT, Arteaga CL. Mutations in the phosphatidylinositol 3-kinase pathway: role in tumor progression and therapeutic implications in breast cancer. *Breast Cancer Res*. 2011;13(6):224.
167. Carraway KL, Theodoropoulos G, Kozloski GA, Carothers Carraway CA. Muc4/MUC4 functions and regulation in cancer. *Future Oncol*. 2009;5(10):1631-40.
168. Chaturvedi P, Singh AP, Moniaux N, Senapati S, Chakraborty S, Meza JL, et al. MUC4 mucin potentiates pancreatic tumor cell proliferation, survival, and invasive properties and interferes with its interaction to extracellular matrix proteins. *Mol Cancer Res*. 2007;5(4):309-20.
169. Ponnusamy MP, Singh AP, Jain M, Chakraborty S, Moniaux N, Batra SK. MUC4 activates HER2 signalling and enhances the motility of human ovarian cancer cells. *Br J Cancer*. 2008;99(3):520-6.
170. Mukhopadhyay P, Lakshmanan I, Ponnusamy MP, Chakraborty S, Jain M, Pai P, et al. MUC4 overexpression augments cell migration and metastasis through EGFR family proteins in triple negative breast cancer cells. *PLoS One*. 2013;8(2):e54455.
171. Nicholson CL, Plautz GE. Cure of Murine Medulloblastoma by Adoptive Transfer of Tumor-Specific T Cells. 2007;110(11):4904-.
172. Clemente CG, Mihm MC, Jr., Bufalino R, Zurrida S, Collini P, Cascinelli N. Prognostic value of tumor infiltrating lymphocytes in the vertical growth phase of primary cutaneous melanoma. *Cancer*. 1996;77(7):1303-10.
173. Vermeulen JF, Van Hecke W, Adriaansen EJM, Jansen MK, Bouma RG, Villacorta Hidalgo J, et al. Prognostic relevance of tumor-infiltrating lymphocytes and immune checkpoints in pediatric medulloblastoma. *Oncoimmunology*. 2018;7(3):e1398877.
174. Rosenberg SA, Yang JC, Sherry RM, Kammula US, Hughes MS, Phan GQ, et al. Durable complete responses in heavily pretreated patients with metastatic melanoma using T-cell transfer immunotherapy. *Clin Cancer Res*. 2011;17(13):4550-7.
175. Rohaan MW, Wilgenhof S, Haanen J. Adoptive cellular therapies: the current landscape. *Virchows Arch*. 2018.
176. Goodman AM, Kato S, Bazhenova L, Patel SP, Frampton GM, Miller V, et al. Tumor Mutational Burden as an Independent Predictor of Response to Immunotherapy in Diverse Cancers. *Mol Cancer Ther*. 2017;16(11):2598-608.

177. McGranahan N, Furness AJ, Rosenthal R, Ramskov S, Lyngaa R, Saini SK, et al. Clonal neoantigens elicit T cell immunoreactivity and sensitivity to immune checkpoint blockade. *Science*. 2016;351(6280):1463-9.
178. Sayour EJ, Mitchell DA. Immunotherapy for Pediatric Brain Tumors. *Brain Sci*. 2017;7(10).
179. Toubaji A, Achta M, Provenzano M, Herrin VE, Behrens R, Hamilton M, et al. Pilot study of mutant ras peptide-based vaccine as an adjuvant treatment in pancreatic and colorectal cancers. *Cancer Immunol Immunother*. 2008;57(9):1413-20.
180. Schuster J, Lai RK, Recht LD, Reardon DA, Paleologos NA, Groves MD, et al. A phase II, multicenter trial of rindopepimut (CDX-110) in newly diagnosed glioblastoma: the ACT III study. *Neuro Oncol*. 2015;17(6):854-61.
181. Verdegaal EM, de Miranda NF, Visser M, Harryvan T, van Buuren MM, Andersen RS, et al. Neoantigen landscape dynamics during human melanoma-T cell interactions. *Nature*. 2016;536(7614):91-5.
182. Chu Y, Liu Q, Wei J, Liu B. Personalized cancer neoantigen vaccines come of age. *Theranostics*. 2018;8(15):4238-46.
183. Carreno BM, Magrini V, Becker-Hapak M, Kaabinejadian S, Hundal J, Petti AA, et al. Cancer immunotherapy. A dendritic cell vaccine increases the breadth and diversity of melanoma neoantigen-specific T cells. *Science*. 2015;348(6236):803-8.
184. Bijker MS, Melief CJ, Offringa R, van der Burg SH. Design and development of synthetic peptide vaccines: past, present and future. *Expert Rev Vaccines*. 2007;6(4):591-603.
185. Quakkelaar ED, Melief CJ. Experience with synthetic vaccines for cancer and persistent virus infections in nonhuman primates and patients. *Adv Immunol*. 2012;114:77-106.
186. Vidard L, Colarusso LJ, Benacerraf B. Specific T-cell tolerance may be preceded by a primary response. *Proc Natl Acad Sci U S A*. 1994;91(12):5627-31.
187. Jenkins MK. The ups and downs of T cell costimulation. *Immunity*. 1994;1(6):443-6.
188. Aichele P, Brduscha-Riem K, Zinkernagel RM, Hengartner H, Pircher H. T cell priming versus T cell tolerance induced by synthetic peptides. *J Exp Med*. 1995;182(1):261-6.
189. Kumai T, Fan A, Harabuchi Y, Celis E. Cancer immunotherapy: moving forward with peptide T cell vaccines. *Curr Opin Immunol*. 2017;47:57-63.
190. Cho HI, Barrios K, Lee YR, Linowski AK, Celis E. BiVax: a peptide/poly-IC subunit vaccine that mimics an acute infection elicits vast and effective anti-tumor CD8 T-cell responses. *Cancer Immunol Immunother*. 2013;62(4):787-99.
191. Gattinoni L, Klebanoff CA, Palmer DC, Wrzesinski C, Kerstann K, Yu Z, et al. Acquisition of full effector function in vitro paradoxically impairs the in vivo antitumor efficacy of adoptively transferred CD8+ T cells. *J Clin Invest*. 2005;115(6):1616-26.
192. Sommermeyer D, Hudecek M, Kosasih PL, Gogishvili T, Maloney DG, Turtle CJ, et al. Chimeric antigen receptor-modified T cells derived from defined CD8+ and CD4+ subsets confer superior antitumor reactivity in vivo. *Leukemia*. 2016;30(2):492-500.
193. Steeber DA, Green NE, Sato S, Tedder TF. Lymphocyte migration in L-selectin-deficient mice. Altered subset migration and aging of the immune system. *J Immunol*. 1996;157(3):1096-106.
194. Lee D, Schultz JB, Knäuf PA, King MR. Mechanical shedding of L-selectin from the neutrophil surface during rolling on sialyl Lewis x under flow. *J Biol Chem*. 2007;282(7):4812-20.
195. Kishimoto TK, Jutila MA, Berg EL, Butcher EC. Neutrophil Mac-1 and MEL-14 adhesion proteins inversely regulated by chemotactic factors. *Science*. 1989;245(4923):1238-41.
196. Fan H, Derynck R. Ectodomain shedding of TGF- α and other transmembrane proteins is induced by receptor tyrosine kinase activation and MAP kinase signaling cascades. *EMBO J*. 1999;18(24):6962-72.
197. E. John Wherry MK. Molecular and cellular insights into T cell exhaustion. *Nat Rev Immunol*. 2015;15:486-99.

G Appendix

1 Supplementary data

Table 9: Overview of donor/peptide combinations tested for *de novo* T-cell responses.

All tested peptides are included, whether they induced a positive T-cell response (+) or not (-). Peptide 15 was tested twice with the same donor, positive in the first and negative in the second run. Peptide 9 and peptide 21 were tested with HLA B*18:01 (a) as well as with B*44:02 (b). Since donor 10 had both HLA types, it is unclear which one mediated the positive response against each peptide (c). P = peptide

	Peptides																					
	P05	P06	P07	P08	P09		P10	P13	P14	P15	P16	P17	P18	P19	P20	P21		P23	P24	P25	P26	
					a	b										a	b					
Donor 01								-			-	-										
Donor 02				-			-		-	+	-		-	-	-	-		-		-	-	
Donor 03	+	-	+																			
Donor 04	-	-	-																			
Donor 05								-				-	-	-	-							
Donor 06											+	-										
Donor 07							-					+		+		-						
Donor 08																		-				
Donor 09							-										-					
Donor 10					+	c	-						-			+	c					
Donor 11							-				-	-					-					
Donor 12	-	-	-																			
Donor 13																				-		
Donor 14							-											-				
Donor 15										-					-							
Donor 16				-						-											+	-
Donor 17								-											-			
Donor 18				-																	-	-

2 Acknowledgements

Ich danke meinem Doktorvater Professor Feuchtinger für die Überlassung des Themas und das Vertrauen, und ebenfalls für die von ihm organisierten oder unterstützten Labortreffen, die die ganze Laborzeit auch privat zu so einer wirklich besonderen Epoche für mich gemacht haben.

Besonderer Dank geht an meine Betreuerin Franziska Blaeschke, die immer ein Ohr für mich hatte, egal ob "in kurzen Worten" und per Sprachnachricht formuliert oder spätabends ermüdet aus dem FACS-Raum oder beides, und die immer gute, schnelle, praktische und funktionierende Ideen und Lösungen hatte.

Außerdem danke ich Theresa Käuferle, die, obwohl andere Doktoranden zu betreuen, unglaublich hilfsbereit war und die, da ebenfalls so nachaktiv wie ich, mit mir so manche lange Laborsession mit einem gemütlichen Kubus-Abendessen aus- oder zwischenklingen ließ.

Ein Mega-Dank an Nadine Stoll, Tanja Weißer und Tanja Roßmann-Bloeck. Nadine, die ein unbeschriebenes, planloses, viel fragendes Blatt in einen Ficoll- und ICS-Routinier verwandeln musste und konnte. Tanja und Tanja, die mit ihrer Assistenz immer zur Stelle und eine große Hilfe waren.

Danke auch an die anderen „Feuchtis“, die ich als Kollegen aber auch als Freunde sehr schätze und mit denen wir an verschiedensten Orten die lustigsten Zeiten verbracht haben.

Vielen Dank an Prof. Martin Schuhmann für die Bereitstellung der Tumorproben, Dr. Christopher Schröder, Dr. Nicolas Casadei und Sven Poths für die Neoepitop-Identifikation, Christopher Mohr für die Bindungsaffinitäts-Berechnung und Prof. Stefan Stevanović für die Peptidsynthese. Danke auch für die wiederholten telefonischen geduldigen Erklärungen zu doch nicht ganz so simplen Verfahren.

Ein großer Dank gilt Prof. Ramin Lotfi, der uns unermüdlich wöchentlich Buffy Coats im IC-Kurier aus Ulm zukommen ließ, ohne die das Projekt nicht möglich gewesen wäre und der uns außerdem mit humanem Serum beliefert hat. Danke an all die gesunden Spender, die sich für das Projekt haben HLA-typisieren und piksen lassen, sowohl in Ulm als auch in München.

Herzlichen Dank an Dr. Beate Wagner und Dr. Georg Wittmann für die wöchentliche Bereitstellung des Gamma-Bestrahlungsgeräts und außerdem ein Dankeschön für die Versorgung mit sogenannten Blutkegeln.

Am Schluss danke ich meiner Familie und meinen Freunden, die mir in der Laborzeit wie auch weiterhin Freude und Unterstützung gaben und geben. Ob Chill, Grill und Splash mit der Münchner Family, Tetris und Tiramisu im Hinterhof mit Freundin und Patenkind, heiße Basketballfights mit dem Mitbewohner, Zeiträtsel-Marathons mit Bruder und Schwägerin, Kochen mit der Schwester, Tatort mit den Eltern, knappe Tawlah-Kämpfe mit dem Studienfreund, Hochhalten auf der Neckarwiese mit dem Schulfreund, alles das und außerdem alle hier ungenannten Highlights machen mir das Leben schön und dafür danke ich euch!



Eidesstattliche Versicherung

Paul, Milan

Name, Vorname

Adresse

Ich erkläre hiermit an Eides statt, dass ich die vorliegende Dissertation mit dem Thema

Induction of T-cell responses against mutation-specific peptides from malignant pediatric brain tumor samples

selbständig verfasst, mich außer der angegebenen keiner weiteren Hilfsmittel bedient und alle Erkenntnisse, die aus dem Schrifttum ganz oder annähernd übernommen sind, als solche kenntlich gemacht und nach ihrer Herkunft unter Bezeichnung der Fundstelle einzeln nachgewiesen habe.

Ich erkläre des Weiteren, dass die hier vorgelegte Dissertation nicht in gleicher oder in ähnlicher Form bei einer anderen Stelle zur Erlangung eines akademischen Grades eingereicht wurde.

München, 28.10.20

Ort, Datum

Milan Paul

Unterschrift Doktorandin/Doktorand